Mon. Not. R. Astron. Soc. **357,** 497–517 (2005) doi:10.1111/j.1365-2966.2005.08609.x

# Kinematics of W Ursae Majoris type binaries and evidence of the two types of formation

S. Bilir,[1⋆] Y. Karataş,[1] O. Demircan[2]† and Z. Eker[2]†

[1]*Istanbul University Science Faculty, Department of Astronomy and Space Sciences, 34119, University-Istanbul, Turkey*
[2]*Çanakkale University, Ulupınar Astrophysical Observatory, 17100 Çanakkale, Turkey*

Accepted 2004 November 5. Received 2004 November 5; in original form 2004 April 26

**ABSTRACT**

We study the kinematics of 129 W UMa binaries and we discuss its implications on the contact binary evolution. The sample is found to be heterogeneous in the velocity space. That is, kinematically younger and older contact binaries exist in the sample. A kinematically young (0.5 Gyr) subsample (moving group) is formed by selecting the systems that satisfy the kinematical criteria of moving groups. After removing the possible moving group members and the systems that are known to be members of open clusters, the rest of the sample is called the field contact binary (FCB) group. The FCB group is further divided into four groups according to the orbital period ranges. Then, a correlation is found in the sense that shorter-period less-massive systems have larger velocity dispersions than the longer-period more-massive systems. Dispersions in the velocity space indicate a 5.47-Gyr kinematical age for the FCB group. Compared with the field chromospherically active binaries (CABs), presumably detached binary progenitors of the contact systems, the FCB group appears to be 1.61 Gyr older. Assuming an equilibrium in the formation and destruction of CAB and W UMa systems in the Galaxy, this age difference is treated as an empirically deduced lifetime of the contact stage. Because the kinematical ages (3.21, 3.51, 7.14 and 8.89 Gyr) of the four subgroups of the FCB group are much longer than the 1.61-Gyr lifetime of the contact stage, the pre-contact stages of the FCB group must dominantly be producing the large dispersions. The kinematically young (0.5 Gyr) moving group covers the same total mass, period and spectral ranges as the FCB group. However, the very young age of this group does not leave enough room for pre-contact stages, and thus it is most likely that these systems were formed in the beginning of the main sequence or during the pre-main-sequence contraction phase, either by a fission process or most probably by fast spiralling in of two components in a common envelope.

**Key words:** binaries: eclipsing – binaries spectroscopic – stars: evolution – stars: kinematics.

## 1 INTRODUCTION

Low-mass contact binaries, popularly known as W Ursae Majoris (W UMa) stars, are easily recognized by their eclipsing light curves with equal (or nearly equal) minima so wide as to touch one another. With a small orbit implied by a short orbital period less than a day, the binary components fill their Roche lobes so that the dumbbell-shaped stars touch each other at the inner Lagrangian point. The W UMa systems have spectral types ranging from late A to middle K and they are located near or just above the main sequence. The strong tidal interaction synchronizes their rotation, and thus the period of rotation is equal to the orbital revolution. The rapid rotation and convective atmospheres are primary causes of their observed chromospheric and coronal emissions as well as the presence of large star-spots, which are the manifestations of strong, dynamo-generated magnetic activity.

The rapid rotation and quickly changing radial velocity, on the other hand, are serious obstacles to obtaining a reliable radial velocity from the highly broadened and blended spectral lines of numerous W UMa systems. Therefore, the formation of a complete sample for studying the galactic space motions and kinematics of W UMa stars is limited by the availability of radial velocity measurements. From the identified 374 W UMa binaries (Kukarkin et al. 1971; van't Veer 1975) in the Third General Catalogue of Variable Stars (GCVS), Guinan & Bradstreet (1988) were able to collect only 34 systems with a measured centre of mass velocity. The number of stars classified as EW (eclipsing binaries of W UMa type) increased to 561 in the fourth edition of the GCVS. However, there were only

⋆E-mail: sbilir@istanbul.edu.tr
†Visiting Astronomer, Istanbul University Science Faculty, Department of Astronomy and Space Sciences.

© 2005 RAS

Downloaded from https://academic.oup.com/mnras/article/357/2/497/1370601 by Akdeniz University user on 20 September 2021

78 systems available with complete physical parameters that were studied statistically by Maceroni & van't Veer (1996). Only 37 out 78 had a spectroscopic mass ratio determined from the radial velocities. Finally, Aslan et al. (1999) counted 125 W UMa binaries in the *Hipparcos* Catalogue, but there were only 34 binaries from which the space motions could be computed. The revised fourth edition of the GCVS now contains 751 W UMa. It is thanks to the dedication of the David Dunlap Observatory (DDO), where 54 per cent of current radial velocities come from, and of the Dominion Astrophysical Observatory (DAO), with a 20 per cent contribution, and to the improvements of spectroscopic techniques for measuring radial velocities that a total of 129 W UMa systems were collected for this study. Nearly four times the amount of data and the improved accuracy of the data justified repeating the previous attempts to study the kinematics of W UMa binaries.

With a small sample of less accurate data, Guinan & Bradstreet (1988) estimated a kinematical age of 8–10 Gyr for W UMa systems. If this age is compared to the ∼5 Gyr average age of chromospherically active binaries (CABs), classical RS CVn and BY Dra systems (Eker 1992), W UMa stars appear two times older. Nevertheless, this age of W UMa binaries was found to be consistent with the theory of contact binary formation from the detached binary progenitors, presumably from the short-period ($P < 5$ d) RS CVn binaries, by a mechanism involving angular momentum loss and orbital period decrease previously suggested by Huang (1967), Mestel (1968), Okamoto & Sato (1970), van't Veer (1979) and Vilhu & Rahunen (1980). However, according to the space velocities and dispersions computed by Aslan et al. (1999), W UMa binaries cannot be older than RS CVn systems. This means that W UMa binaries could not have evolved from detached binaries, unless the time to reach contact stage is very short.

With no pre-contact stage, there is an opposing theory which predicts the formation of contact binaries directly by a fission process (Roxburgh 1966) at the end of the pre-main-sequence contraction. Considering the brief lifetime of the contact stage ($0.1 < t_{\rm contact} < 1$ Gyr) estimated by Guinan & Bradstreet (1988), this theory would fail to produce older populations of W UMa binaries unless the angular momentum of contact binaries is conserved. However, with the conservation of the orbital angular momentum, this theory would refute the formation of the contact binaries from the detached binary progenitors.

Apparently, empirical evidence implying whether the total orbital angular momentum is conserved or not within the evolutionary timescale is extremely important in order to reveal the actual working model. Inspired by the predictions of Demircan (1999), Karataş et al. (2004) presented such evidence recently from the kinematics of a CAB sample containing RS CVn and BY Dra stars. The evidence of orbital period decrease, connected to mass and angular momentum loss, was shown by comparing the total mass ($M_1 + M_2$) and period histograms between the kinematically younger (age 0.95 Gyr) and the older (age 3.86 Gyr) CAB subsamples. The orbital period decrease was also indicated by the fact that the shorter orbital period systems were found to be older than the longer orbital period systems. According to a preliminary investigation by Demircan et al. (in preparation), the period decrease is exponential in time so that the active detached binaries, up to about 5-d orbital period, could change into contact form within less than about 5 Gyr. Therefore, the formation of W UMa stars from detached binaries is evidently occurring. Nevertheless, this does not mean this is the only mechanism by which contact binaries are formed. It may still possible that a limited fraction of W UMa systems, possibly the very young ones, may be forming by the fission process.

In the present work, we study the kinematics of W UMa binaries and we discuss its implications on the contact binary evolution. The present sample has been found to be heterogeneous, like the CAB sample, in the sense that there are younger (age ∼1 Gyr) and older (age ∼6 Gyr) W UMa binaries covering the same range of spectral types and orbital periods. The evidence of mass and angular momentum loss causing orbital period decrease during contact binary evolution has been investigated as a preliminary step, as done for the CAB sample by Karataş et al. (2004), by comparing the total mass ($M_1 + M_2$) and period histograms between the younger and the older subsamples.

## 2 DATA

Among the 751 recorded W UMa binaries in the recently revised fourth edition of the GCVS, 129 systems were found to have radial velocities. After compiling the rest of the basic data (parallaxes and proper motions), the sample is listed in Table 1, which is self-explanatory, with the columns giving the order number, name, HD and *Hipparcos* reference numbers, celestial coordinates [International Celestial Reference System (ICRS) 2000], proper motions, parallaxes and radial velocities. The associated standard errors are given beside the related parameter. The reference numbers in the last column are separated by semicolons into three fields to indicate where the basic data were taken from. The two or more reference numbers in a field indicate the subfields, i.e. there are multiple references.

### 2.1 Parallaxes and proper motions

The parallaxes and the proper motions in Table 1 were mostly taken from the *Hipparcos* and Tycho Catalogues (ESA 1997) and the Tycho Reference Catalogue (Hog et al. 1998). The parallax and the proper motion components of three stars (TX Cnc, EE Cet, BL Eri) were taken from Roese & Bastian (1988). Among the 129 systems in Table 1, 25 binaries do not have any trigonometric parallax and 12 binaries have a large relative uncertainty ($\sigma_\pi/\pi > 0.5$) in the parallax measurements. Considering the fact that the *Hipparcos* measurements are reliable up to 500 pc ($2\sigma$ detection limit $\sigma \approx 1$ mas; Perryman et al. 1997), we decided to discard the parallaxes of five systems (AQ Tuc, TY Pub, XZ Leo, AG Vir, RZ Com) because their measured parallaxes indicate a distance further than 500 pc. These five stars and ER Ori, which were erroneously listed with a negative parallax, are treated like the other 25 systems without a trigonometric parallax. For these, we used the photometric parallaxes, which were determined from the period–colour–brightness relation $M(V) = -4.44 \log P + 3.02(B–V)_{\rm o} + 0.12$ by Rucinski (2004). The photometric parallaxes were calculated with the corrections of the interstellar absorption, which were computed from the colour excess as $A_V = 3.1\,E(B–V)$. Because all systems were assigned a spectral type, the colour excesses were available, together with their observed colours.

The *Hipparcos* and Tycho Catalogues usually give an associated uncertainty for all of the parallax and the proper motion component measurements. However, there are 18 systems in the list without an uncertainty at the proper motion component. With an optimistic approach, we have preferred to adopt an average uncertainty of 2.5 mas yr$^{-1}$ for these, as determined by Hog et al. (2000) for the *Hipparcos* stars in general. On the other hand, Rucinski (2004) estimated that the absolute magnitudes computed using the period–brightness relation of W UMa systems are within an accuracy of ±0.25 mag.



Downloaded from https://academic.oup.com/mnras/article/357/2/497/1370601 by Akdeniz University user on 20 September 2021

**Table 1.** *Hipparcos* astrometric and radial velocity data of the W UMas. The references are as follows: 1, Perryman et al. (1997); 2, Hog et al. (2000); 3, Roese & Bastian (1988); 4, Hog et al. (1998); 5, Rucinski (2004); 6, Hilditch & King (1986); 7, Metcalfe (1999); 8, Rucinski et al. (2003); 9, Maceroni (1986); 10, Milone, Hrivnak & Fisher (1985b); 11, Lu & Rucinski (1999); 12, Duerbeck (1978); 13, Struve et al. (1950); 14, Rucinski et al. (2001); 15, Milone et al. (1995); 16, Lu (1991); 17, Rucinski et al. (2002); 18, Rucinski, Lu & Mochnacki (2000); 19, Yamasaki, Jugaku & Seki (1988); 20, Nesci et al. (1986); 21, Pych et al. (2004); 22, Przybylski & Morris (1965); 23, Goecking et al. (1994); 24, Hilditch, Hill & Bell (1992); 25, Lu (1993); 26, Rucinski & Lu (1999); 27, Struve (1950); 28, McLean & Hilditch (1983); 29, Whelan et al. (1979); 30, King & Hilditch (1984); 31, Joy (1926); 32, Rucinski, Lu & Shi (1993); 33, Lu (1988a); 34, Hrivnak et al. (1984); 35, Lu, Rucinski & Ogloza (2001); 36, Hrivnak (1993); 37, Moore & Paddock (1950); 38, McLean (1981); 39, Hilditch, King & McFarlane (1989); 40, Sistero & Castore de Sistero (1974); 41, Hill & Barnes (1972); 42, Rucinski, Whelan & Worden (1977); 43, Lu & Rucinski (1993); 44, Milone et al. (1985a); 45, Lu (1988b); 46, Cerruti & Niemela (1982); 47, Rainger, Bell & Hilditch (1990b); 48, Rainger, Hilditch & Bell (1990a); 49, Batten & Lu (1986); 50, Sanford (1934); 51, Nelson et al. (1995); 52, Schoeffel (1979); 53, McLean (1983); 54, Lu (1986); 55, Pazhouhesh & Edalati (2003); 56, Goecking & Duerbeck (1993); 57, Hrivnak (1989); 58, Bell, Rainger & Hilditch (1990); 59, Hill (1989); 60, Ahn, Hill & Khalesseh (1992); 61, Samec & Hube (1991); 62, Zhai & Lu (1989); 63, Hrivnak & Milone (1989); 64, Maciejewski, Ligeza & Karska (2003); 65, Lu (1985); 66, Hill, Fisher & Holmgren (1989); 67, Montgomery, Marschall & Janes (1993); 68, Gatewood & de Jonge (1994); 69, Gatewood (1995).

| ID | Name | HD | HIP | $\alpha$ (2000) ($^{\rm h}\,^{\rm m}\,^{\rm s}$) | $\delta$(2000) ($^\circ\,'\,''$) | $\mu_\alpha \cos\delta$ (mas yr$^{-1}$) | | $\mu_\delta$ (mas yr$^{-1}$) | | $\pi$ (mas) | | $\gamma$ (km s$^{-1}$) | | Refs |
|---|---|---|---|---|---|---|---|---|---|---|---|---|---|---|
| 1 | AQ Tuc | 1372 | 1387 | 00 17 21.51 | −71 54 56.84 | 28.37 | 1.20 | −9.37 | 1.10 | 2.84 | 0.36 | 20.60 | 0.27 | (1;5;6) |
| 2 | BH Cas | | | 00 21 40.30 | +59 12 06.60 | −7.43 | 2.50 | −32.18 | 2.50 | 3.37 | 0.42 | −23.70 | 2.40 | (2;5;7) |
| 3 | DZ Psc | | | 00 36 27.93 | +21 32 13.60 | −6.30 | 2.50 | 14.90 | 2.50 | 4.83 | 0.60 | −21.66 | 2.15 | (2;5;8) |
| 4 | V523 Cas | | | 00 40 06.26 | +50 14 15.53 | 146.00 | 2.60 | −71.10 | 2.50 | 12.44 | 1.56 | −2.54 | 0.90 | (2;5;8;9;10) |
| 5 | AQ Psc | 8152 | 6307 | 01 21 03.56 | +07 36 21.63 | −8.72 | 1.38 | 14.58 | 0.73 | 8.03 | 1.29 | −12.90 | 0.40 | (1;1;11) |
| 6 | AE Phe | 9528 | 7183 | 01 32 32.93 | −49 31 41.29 | 150.93 | 0.80 | −54.47 | 0.65 | 20.49 | 0.81 | −9.50 | 2.50 | (1;1;12) |
| 7 | TW Cet | | 8447 | 01 48 54.14 | −20 53 34.60 | 44.82 | 3.69 | −15.91 | 2.18 | 9.91 | 3.50 | 20.00 | 25.0 | (1;1;13) |
| 8 | V776 Cas | | 8821 | 01 53 23.44 | +70 02 33.44 | 19.44 | 1.51 | 4.32 | 1.07 | 4.86 | 1.56 | −24.71 | 0.69 | (1;1;14) |
| 9 | QX And | | | 01 57 57.10 | +37 48 23.00 | 12.10 | 2.50 | −11.50 | 2.50 | 2.63 | 0.23 | 11.70 | 0.27 | (2;15;15) |
| 10 | SS Ari | | | 02 04 18.41 | +24 00 02.23 | 25.60 | 2.50 | −10.70 | 2.50 | 4.71 | 0.59 | −3.20 | 1.30 | (2;5;16) |
| 11 | GZ And | | 10270 | 02 12 14.07 | +44 39 36.28 | −15.40 | 2.50 | −0.60 | 2.50 | 6.15 | 0.77 | 0.00 | 1.20 | (2;5;11) |
| 12 | V376 And | 15922 | 12039 | 02 35 11.63 | +49 51 37.20 | 49.40 | 0.86 | −8.28 | 0.66 | 5.07 | 0.89 | 22.83 | 0.89 | (1;1;14) |
| 13 | EE Cet | 17613 | 13199 | 02 49 52.38 | +08 56 22.63 | 45.90 | 5.00 | −1.00 | 4.90 | 7.29 | 0.91 | 1.60 | 0.93 | (3;5;17) |
| 14 | UX Eri | | 14699 | 03 09 52.74 | −06 53 33.56 | 24.13 | 2.85 | −3.80 | 1.91 | 6.57 | 2.84 | 12.79 | 1.09 | (1;1;18) |
| 15 | EQ Tau | | | 03 48 13.43 | +22 18 50.94 | 68.40 | 2.50 | −29.60 | 2.50 | 6.97 | 0.87 | 71.95 | 1.22 | (2;5;14) |
| 16 | BL Eri | | | 04 11 48.18 | −11 47 26.52 | 11.70 | 2.70 | 1.00 | 2.70 | 2.77 | 0.35 | 40.00 | 1.51 | (3;5;19) |
| 17 | YY Eri | 26609 | 19610 | 04 12 08.85 | −10 28 09.96 | −111.87 | 1.46 | −114.52 | 0.96 | 17.96 | 1.20 | −15.00 | 1.50 | (1;1;20) |
| 18 | AO Cam | | | 04 28 13.64 | +53 02 44.52 | 14.80 | 2.50 | −23.30 | 2.50 | 9.20 | 1.15 | −13.17 | 0.83 | (2;5;18) |
| 19 | RZ Tau | 285892 | 21467 | 04 36 37.66 | +18 45 17.80 | −26.31 | 1.76 | −6.42 | 1.28 | 5.74 | 1.85 | 5.00 | 50.0 | (1;1;13) |
| 20 | DN Cam | 29213 | 21913 | 04 42 46.24 | +72 58 41.87 | −17.90 | 0.80 | −12.98 | 0.50 | 4.49 | 0.89 | 6.04 | 0.98 | (1;1;14) |
| 21 | V410 Aur | 280332 | 23337 | 05 01 10.84 | +34 30 26.57 | 9.04 | 4.97 | −5.33 | 2.99 | 4.77 | 5.39 | 36.94 | 3.10 | (1;1;8) |
| 22 | V402 Aur | 282719 | 23433 | 05 02 14.74 | +31 15 49.29 | 9.68 | 1.58 | −5.84 | 1.05 | 7.01 | 1.31 | 40.82 | 0.93 | (1;1;21) |
| 23 | AP Dor | 33474 | 23793 | 05 06 45.09 | −59 03 03.45 | 56.68 | 1.23 | 77.85 | 0.73 | 4.66 | 0.92 | 6.80 | 0.97 | (1;1;22) |
| 24 | V1363 Ori | 289949 | 23809 | 05 07 02.11 | −00 47 32.64 | 21.99 | 2.27 | −42.58 | 1.50 | 9.47 | 2.36 | 37.89 | 2.02 | (1;1;21) |
| 25 | ER Ori | | 24156 | 05 11 14.50 | −08 33 24.66 | 7.20 | 1.71 | −25.73 | 1.14 | 6.24 | 0.78 | 37.90 | 3.30 | (1;5;23) |
| 26 | RW Dor | 269320 | 24763 | 05 18 32.54 | −68 13 32.76 | 96.63 | 2.57 | 55.06 | 1.86 | 8.91 | 1.97 | 66.50 | 1.45 | (1;1;24) |
| 27 | V781 Tau | 248087 | 27562 | 05 50 13.12 | +26 57 43.37 | −81.59 | 1.51 | −85.08 | 0.77 | 12.31 | 1.35 | 24.40 | 1.30 | (1;1;25) |
| 28 | AH Aur | 256902 | 30618 | 06 26 04.90 | +27 59 56.40 | 15.21 | 2.23 | −12.72 | 1.36 | 6.18 | 2.05 | 31.95 | 1.45 | (1;1;26) |
| 29 | QW Gem | 264672 | 32845 | 06 50 46.07 | +29 27 11.34 | 16.57 | 8.12 | −22.58 | 2.97 | 4.09 | 5.42 | −0.90 | 1.39 | (1;1;8) |
| 30 | V753 Mon | 54975 | 34684 | 07 10 57.85 | −03 52 43.19 | −13.56 | 0.98 | −9.14 | 0.66 | 5.23 | 1.04 | 38.58 | 0.83 | (1;1;18) |
| 31 | TY Pup | 60265 | 36683 | 07 32 46.23 | −20 47 31.07 | −24.05 | 1.09 | 42.09 | 0.76 | 4.67 | 0.58 | 28.00 | 30.0 | (1;5;27) |
| 32 | FG Hya | | 41437 | 08 27 03.94 | +03 30 52.33 | 6.88 | 1.92 | −63.68 | 1.40 | 2.92 | 1.90 | −5.70 | 1.20 | (1;1;11) |
| 33 | TX Cnc | | | 08 40 01.67 | +18 59 58.72 | −48.20 | 4.00 | −19.00 | 3.90 | 5.21 | 0.79 | 29.00 | 2.12 | (3;68;28) |
| 34 | AH Cnc | | | 08 51 37.87 | +11 50 57.20 | −7.80 | 2.50 | −9.10 | 2.50 | 1.20 | 0.10 | 15.00 | 1.89 | (2;67;29) |
| 35 | UV Lyn | | 44455 | 09 03 24.12 | +38 05 54.60 | −71.67 | 1.79 | 18.85 | 1.02 | 8.16 | 1.62 | −0.30 | 1.30 | (1;1;11) |
| 36 | FN Cam | 79886 | 46005 | 09 22 58.04 | +77 13 10.95 | −4.31 | 1.13 | −28.56 | 0.74 | 3.62 | 0.95 | 12.96 | 1.11 | (1;1;14) |
| 37 | EZ Hya | | | 09 26 41.06 | −13 45 06.41 | −30.80 | 3.30 | −0.30 | 2.50 | 5.43 | 0.68 | 16.00 | 0.44 | (4;5;30) |
| 38 | S Ant | 82610 | 46810 | 09 32 18.39 | −28 37 39.97 | −88.84 | 0.55 | 43.79 | 0.49 | 13.30 | 0.71 | −5.00 | 1.80 | (1;1;31) |
| 39 | W UMa | 83950 | 47727 | 09 43 45.47 | +55 57 09.08 | 15.55 | 1.03 | −27.35 | 0.62 | 20.17 | 1.05 | −29.60 | 1.22 | (1;1;32) |
| 40 | AA UMa | | | 09 46 59.29 | +45 45 56.40 | −1.00 | 2.50 | −4.80 | 2.50 | 3.19 | 0.40 | −34.80 | 1.90 | (2;5;33) |
| 41 | RT Lmi | | | 09 49 48.32 | +34 27 15.40 | 3.60 | 2.50 | −6.00 | 2.50 | 3.07 | 0.38 | −10.30 | 1.74 | (2;5;18) |
| 42 | XY Leo | | 49136 | 10 01 40.43 | +17 24 32.70 | 56.70 | 1.68 | −58.27 | 0.71 | 15.86 | 1.80 | −50.00 | 2.00 | (1;1;34) |
| 43 | XZ Leo | | 49204 | 10 02 34.19 | +17 02 47.14 | −16.10 | 1.78 | 1.85 | 0.81 | 2.59 | 0.32 | −2.03 | 1.43 | (1;5;26) |
| 44 | Y Sex | 87079 | 49217 | 10 02 47.96 | +01 05 40.35 | 0.67 | 3.84 | −2.67 | 2.05 | 9.02 | 3.38 | 9.80 | 2.00 | (1;1;28) |
| 45 | ET Leo | 91386 | 51677 | 10 33 25.79 | +17 34 27.43 | −37.71 | 1.53 | −7.21 | 0.80 | 13.90 | 1.44 | 21.46 | 0.78 | (1;1;17) |
| 46 | UZ Leo | | 52249 | 10 40 33.19 | +13 34 00.86 | −21.60 | 1.49 | −1.10 | 0.89 | 6.27 | 1.59 | −8.18 | 1.12 | (1;1;26) |
| 47 | EX Leo | 93077 | 52580 | 10 45 06.77 | +16 20 15.68 | −26.51 | 1.23 | −37.11 | 0.75 | 9.84 | 1.11 | −11.05 | 1.10 | (1;1;35) |
| 48 | VY Sex | 93917 | | 10 50 29.72 | −02 41 43.05 | −21.40 | 2.90 | −88.60 | 2.20 | 7.34 | 0.92 | 17.47 | 0.79 | (4;5;8) |
| 49 | AM Leo | | 53937 | 11 02 10.89 | +09 53 42.69 | −9.98 | 4.54 | −29.53 | 3.26 | 13.03 | 3.64 | 5.60 | 1.20 | (1;1;36) |



Downloaded from https://academic.oup.com/mnras/article/357/2/497/1370601 by Akdeniz University user on 20 September 2021

**Table 1** – *continued*

| ID | Name | HD | HIP | $\alpha$ (2000) ($^{h}\,^{m}\,^{s}$) | $\delta$(2000) ($^{\circ}\,'\,''$) | $\mu_\alpha \cos\delta$ (mas yr$^{-1}$) | | $\mu_\delta$ (mas yr$^{-1}$) | | $\pi$ (mas) | | $\gamma$ (km s$^{-1}$) | | Refs |
|---|---|---|---|---|---|---|---|---|---|---|---|---|---|---|
| 50 | VW Lmi | 95660 | 54003 | 11 02 51.91 | +30 24 54.71 | 12.21 | 0.98 | −3.92 | 0.66 | 8.04 | 0.90 | 5.00 | 0.75 | (1;1;37) |
| 51 | AP Leo | | 54188 | 11 05 05.02 | +05 09 06.42 | 89.94 | 2.05 | −59.58 | 1.17 | 8.26 | 1.70 | −25.10 | 2.10 | (1;1;11) |
| 52 | HN UMa | | 55030 | 11 15 56.38 | +37 38 35.30 | 56.12 | 1.28 | −35.67 | 0.90 | 5.81 | 1.39 | −37.11 | 0.63 | (1;1;8) |
| 53 | AW UMa | 99946 | 56109 | 11 30 04.32 | +29 57 52.67 | −82.35 | 0.87 | −199.74 | 0.68 | 15.13 | 0.90 | −17.00 | 1.57 | (1;1;38) |
| 54 | TV Mus | 310730 | | 11 39 57.76 | −64 48 59.29 | 27.00 | 5.20 | −6.80 | 3.20 | 4.32 | 0.54 | 3.10 | 1.00 | (4;5;39) |
| 55 | V752 Cen | 101799 | 57129 | 11 42 48.08 | −35 48 57.51 | −53.65 | 1.63 | −24.28 | 0.93 | 9.51 | 1.47 | 29.10 | 0.82 | (1;1;40) |
| 56 | AG Vir | 104350 | 58605 | 12 01 03.50 | +13 00 30.02 | −2.46 | 1.46 | −17.64 | 0.56 | 5.02 | 0.63 | −5.91 | 0.73 | (1;5;41,58) |
| 57 | HX UMa | 104425 | 58648 | 12 01 33.15 | +43 02 29.94 | 65.86 | 2.56 | −21.34 | 2.15 | 6.68 | 3.01 | −19.88 | 1.11 | (1;1;8) |
| 58 | CC Com | | | 12 12 06.20 | +22 31 58.00 | −120.00 | 2.50 | 19.30 | 2.50 | 12.49 | 1.56 | −10.20 | 1.31 | (2;5;42) |
| 59 | AH Vir | 106400 | 59683 | 12 14 21.00 | +11 49 09.40 | 47.74 | 3.03 | −107.26 | 1.39 | 10.86 | 3.11 | 6.60 | 0.90 | (1;1;43) |
| 60 | II UMa | 109247 | 61327 | 12 32 54.84 | +54 47 42.89 | −42.50 | 1.57 | −12.12 | 1.45 | 5.04 | 1.81 | −8.02 | 1.10 | (1;1;17) |
| 61 | RW Com | | 61243 | 12 33 00.28 | +26 42 58.38 | −125.45 | 3.46 | −36.05 | 1.89 | 11.45 | 2.45 | −53.00 | 1.15 | (1;1;44) |
| 62 | RZ Com | | 61414 | 12 35 05.06 | +23 20 14.02 | 17.44 | 1.79 | −11.01 | 1.18 | 4.70 | 0.59 | −1.80 | 1.67 | (1;5;28) |
| 63 | SX Crv | 110139 | 61825 | 12 40 15.04 | −18 48 00.93 | 37.93 | 1.21 | −5.63 | 0.92 | 10.90 | 1.21 | 8.71 | 0.94 | (1;1;14) |
| 64 | BI CVn | | 63701 | 13 03 16.41 | +36 37 00.59 | −6.38 | 1.23 | −16.68 | 1.04 | 5.31 | 1.65 | −5.30 | 1.80 | (1;1;45) |
| 65 | KZ Vir | 114726 | 64433 | 13 12 22.87 | +02 39 13.78 | −8.53 | 0.98 | 0.94 | 0.48 | 6.53 | 0.93 | −4.50 | 0.48 | (1;1;14) |
| 66 | KR Com | 115955 | 65069 | 13 20 15.78 | +17 45 56.99 | −6.70 | 0.78 | −82.30 | 0.47 | 13.07 | 0.87 | −7.86 | 0.38 | (1;1;17) |
| 67 | HT Vir | 119931 | 67186 | 13 46 06.75 | +05 06 56.27 | −107.79 | 3.24 | −11.16 | 1.68 | 15.39 | 2.72 | −23.38 | 0.68 | (1;1;35) |
| 68 | XY Boo | | 67431 | 13 49 11.57 | +20 11 24.59 | −23.32 | 1.87 | 26.91 | 0.89 | 2.94 | 1.70 | 2.11 | 2.02 | (1;1;28) |
| 69 | V757 Cen | 120734 | 67682 | 13 51 55.74 | −36 37 24.82 | −121.51 | 1.20 | −61.89 | 0.94 | 14.18 | 1.10 | 50.00 | 2.50 | (1;1;46) |
| 70 | RR Cen | 124689 | 69779 | 14 16 57.22 | −57 51 15.65 | −52.69 | 0.77 | −22.37 | 0.57 | 9.76 | 0.85 | −16.00 | 0.41 | (1;1;30) |
| 71 | VW Boo | | 69826 | 14 17 26.03 | +12 34 03.45 | 5.45 | 2.09 | −48.79 | 0.95 | 3.44 | 1.90 | 23.90 | 0.82 | (1;1;47) |
| 72 | NN Vir | 125488 | 70020 | 14 19 37.74 | +05 53 46.66 | −54.17 | 1.09 | −19.63 | 0.60 | 9.48 | 1.14 | −6.24 | 0.65 | (1;1;26) |
| 73 | EF Boo | 234150 | 71107 | 14 32 30.54 | +50 49 40.70 | −33.23 | 1.17 | −37.34 | 0.93 | 6.00 | 1.06 | −13.16 | 1.07 | (1;1;14) |
| 74 | CK Boo | 128141 | 71319 | 14 35 03.76 | +09 06 49.39 | 70.91 | 1.18 | −86.58 | 0.80 | 6.38 | 1.34 | 37.04 | 0.75 | (1;1;26) |
| 75 | GR Vir | 129903 | 72138 | 14 45 20.26 | −06 44 04.13 | −84.94 | 1.47 | 47.34 | 0.99 | 18.83 | 1.18 | −71.72 | 0.89 | (1;1;26) |
| 76 | AC Boo | | 73103 | 14 56 28.34 | +46 21 44.14 | −9.11 | 1.30 | 8.99 | 1.26 | 7.58 | 1.27 | −8.60 | 2.20 | (1;1;36) |
| 77 | TY Boo | | | 15 00 46.94 | +35 07 54.89 | −58.80 | 2.50 | 32.30 | 2.50 | 5.82 | 0.73 | −41.90 | 1.55 | (2;5;48) |
| 78 | 44 Boo | 133640 | 73695 | 15 03 47.30 | +47 39 14.62 | −436.26 | 1.36 | 18.93 | 0.98 | 78.39 | 1.03 | −17.89 | 0.40 | (1;1;35) |
| 79 | TZ Boo | | 74061 | 15 08 09.13 | +39 58 12.86 | −89.03 | 1.53 | 58.80 | 1.42 | 6.76 | 1.49 | −36.70 | 1.51 | (1;1;28) |
| 80 | BW Dra | | 74368 | 15 11 50.11 | +61 51 41.26 | −153.96 | 8.04 | 98.81 | 6.44 | 15.32 | 5.18 | −60.80 | 1.15 | (1;1;49) |
| 81 | BV Dra | 135421 | 74370 | 15 11 50.36 | +61 51 25.32 | −162.57 | 2.98 | 99.13 | 2.47 | 14.86 | 2.56 | −61.45 | 1.45 | (1;1;49) |
| 82 | FI Boo | 234224 | 75203 | 15 22 05.97 | +51 10 55.33 | −36.87 | 2.46 | 47.43 | 2.29 | 9.52 | 2.10 | −30.55 | 0.72 | (1;1;35) |
| 83 | OU Ser | 136924 | 75269 | 15 22 43.47 | +16 15 40.74 | −387.51 | 0.91 | 2.80 | 0.77 | 17.31 | 0.95 | −64.08 | 0.41 | (1;1;18) |
| 84 | VZ Lib | | 76050 | 15 31 51.76 | −15 41 00.19 | −15.61 | 2.55 | −1.94 | 1.75 | 4.92 | 1.96 | −31.11 | 2.30 | (1;1;35) |
| 85 | FU Dra | | 76272 | 15 34 45.21 | +62 16 44.28 | −255.85 | 1.18 | 15.61 | 1.11 | 6.25 | 1.09 | −11.38 | 1.14 | (1;1;18) |
| 86 | YY CrB | 141990 | 77598 | 15 50 32.43 | +37 50 07.56 | −74.09 | 0.92 | 10.93 | 0.71 | 11.36 | 0.85 | −4.58 | 1.02 | (1;1;18) |
| 87 | AU Ser | | | 15 56 49.47 | +22 16 01.59 | −31.40 | 2.50 | −48.60 | 2.50 | 5.46 | 0.68 | −62.90 | 1.50 | (2;5;36) |
| 88 | V842 Her | | | 16 06 02.34 | +50 11 12.10 | −27.90 | 2.50 | 20.70 | 2.50 | 6.08 | 0.76 | −57.98 | 1.55 | (2;5;26) |
| 89 | BX Dra | | 78891 | 16 06 17.37 | +62 45 46.10 | −7.80 | 1.11 | 7.55 | 0.92 | 3.38 | 1.15 | −26.11 | 3.43 | (1;1;21) |
| 90 | V899 Her | 149684 | 81191 | 16 35 01.96 | +33 12 47.77 | 39.09 | 0.72 | −39.57 | 0.55 | 8.06 | 0.77 | −16.84 | 1.30 | (1;1;35) |
| 91 | V502 Oph | 150484 | 81703 | 16 41 20.86 | +00 30 27.37 | −27.95 | 1.76 | 20.92 | 0.86 | 11.84 | 1.17 | −42.56 | 0.85 | (1;1;21) |
| 92 | V918 Her | 151701 | 82253 | 16 48 24.18 | +17 07 59.63 | −15.88 | 0.88 | 14.27 | 0.62 | 8.70 | 0.93 | −25.72 | 0.74 | (1;1;21) |
| 93 | V921 Her | 152172 | 82344 | 16 49 31.24 | +47 06 28.81 | 7.46 | 0.98 | 5.15 | 0.91 | 2.39 | 0.97 | −79.04 | 1.05 | (1;1;8) |
| 94 | V829 Her | | | 16 55 47.88 | +35 10 57.60 | −11.80 | 3.10 | −15.60 | 2.60 | 13.53 | 0.54 | −13.40 | 1.00 | (4;69;11) |
| 95 | V2357 Oph | | 82967 | 16 57 16.76 | +10 59 51.38 | 0.51 | 1.80 | −103.60 | 1.11 | 5.37 | 2.01 | −19.12 | 1.64 | (1;1;8) |
| 96 | AK Her | 155937 | 84293 | 17 13 57.82 | +16 21 00.61 | 26.24 | 2.23 | −47.63 | 1.99 | 10.47 | 2.77 | −13.00 | 15.0 | (1;1;50) |
| 97 | V728 Her | | | 17 18 04.46 | +41 50 40.40 | −14.40 | 2.50 | −10.10 | 2.50 | 2.41 | 0.30 | 34.40 | 0.80 | (2;5;51) |
| 98 | GM Dra | 238677 | 84837 | 17 20 21.88 | +57 58 27.00 | 77.21 | 1.13 | −59.05 | 1.02 | 10.16 | 0.88 | 9.12 | 1.63 | (1;1;17) |
| 99 | V2377 Oph | 159356 | 85944 | 17 33 56.05 | +08 09 57.81 | −12.87 | 1.00 | −59.16 | 0.72 | 10.09 | 1.22 | −25.79 | 0.38 | (1;1;35) |
| 100 | V535 Ara | 159441 | 86306 | 17 38 05.55 | −56 49 17.29 | −76.64 | 0.90 | −49.51 | 0.50 | 8.87 | 0.90 | −17.60 | 0.60 | (1;1;52) |
| 101 | V2388 Oph | 163151 | 87655 | 17 54 14.17 | +11 07 50.01 | −70.81 | 0.87 | −163.11 | 0.50 | 14.72 | 0.81 | −25.88 | 0.52 | (1;1;17) |
| 102 | V566 Oph | 163611 | 87860 | 17 56 52.41 | +04 59 15.32 | 54.04 | 1.17 | 73.92 | 0.77 | 13.98 | 1.11 | −42.95 | 1.13 | (1;1;53,66) |
| 103 | V972 Her | 164078 | 87958 | 17 58 05.00 | +32 38 53.02 | −34.42 | 0.51 | −28.43 | 0.46 | 16.25 | 0.61 | 3.98 | 0.46 | (1;1;17) |
| 104 | V508 Oph | | 88028 | 17 58 48.62 | +13 29 46.27 | −14.62 | 1.88 | −45.07 | 1.38 | 7.68 | 2.14 | −36.40 | 2.05 | (1;1;54) |
| 105 | EF Dra | | | 18 05 30.48 | +69 45 15.71 | −13.60 | 2.70 | −24.40 | 2.40 | 5.74 | 0.72 | −42.20 | 3.50 | (4;5;11) |
| 106 | V839 Oph | 166231 | 88946 | 18 09 21.27 | +09 09 03.63 | −32.48 | 1.33 | 3.23 | 1.03 | 8.09 | 1.44 | −63.76 | 0.32 | (1;1;55) |
| 107 | eps Cra | 175813 | 93174 | 18 58 43.38 | −37 06 26.48 | −132.25 | 1.46 | −110.45 | 0.55 | 33.43 | 0.92 | 57.90 | 1.20 | (1;1;56) |
| 108 | V401 Cyg | | 95816 | 19 29 20.27 | +30 24 28.48 | −4.96 | 8.70 | −12.59 | 5.99 | 11.55 | 8.04 | 25.53 | 2.14 | (1;1;17) |
| 109 | V2082 Cyg | 183752 | 95833 | 19 29 30.07 | +36 17 14.93 | 20.17 | 0.53 | 94.83 | 0.50 | 11.04 | 0.56 | −34.12 | 0.58 | (1;1;21) |
| 110 | V417 Aql | | 96349 | 19 35 24.12 | +05 50 17.66 | −1.90 | 2.86 | −24.45 | 1.50 | 7.65 | 2.35 | −14.20 | 1.40 | (1;1;11) |
| 111 | OO Aql | 187183 | | 19 48 12.65 | +09 18 32.38 | 65.70 | 1.60 | −7.90 | 1.60 | 6.52 | 0.82 | −45.20 | 0.90 | (4;5;57) |

Downloaded from https://academic.oup.com/mnras/article/357/2/497/1370601 by Akdeniz University user on 20 September 2021

**Table 1** – *continued*

| ID | Name | HD | HIP | $\alpha$ (2000) ($^{\rm h}\,^{\rm m}\,^{\rm s}$.) | $\delta$(2000) ($^\circ\,'\,''$.) | $\mu_\alpha \cos\delta$ (mas yr$^{-1}$) | | $\mu_\delta$ (mas yr$^{-1}$) | | $\pi$ (mas) | | $\gamma$ (km s$^{-1}$) | | Refs |
|---|---|---|---|---|---|---|---|---|---|---|---|---|---|---|
| 112 | VW Cep | 197433 | 101750 | 20 37 21.54 | +75 36 01.46 | 309.23 | 1.12 | 539.47 | 0.97 | 36.16 | 0.97 | −7.90 | 1.00 | (1;1;59) |
| 113 | LS Del | 199497 | | 20 57 10.29 | +19 38 59.23 | 145.40 | 1.90 | 83.40 | 1.80 | 12.71 | 1.59 | −25.90 | 1.40 | (4;5;11) |
| 114 | V2150 Cyg | 202924 | 105162 | 21 18 10.88 | +30 35 21.58 | 2.58 | 1.27 | −6.25 | 0.91 | 4.73 | 1.59 | −12.82 | 0.45 | (1;1;35) |
| 115 | HV Aqr | | | 21 21 24.81 | −03 09 36.88 | −63.50 | 1.90 | −92.30 | 1.80 | 6.99 | 0.87 | −3.77 | 1.25 | (4;5;18) |
| 116 | V1073 Cyg | 204038 | 105739 | 21 25 00.36 | +33 41 14.94 | −4.70 | 2.50 | −21.00 | 2.50 | 5.44 | 0.95 | −0.80 | 1.10 | (2;1;60) |
| 117 | KP Peg | 204215 | 105882 | 21 26 41.13 | +13 41 17.75 | −2.31 | 2.40 | −10.65 | 1.20 | 4.37 | 1.67 | 5.52 | 1.03 | (1;1;21) |
| 118 | DK Cyg | | 106574 | 21 35 02.67 | +34 35 45.40 | −28.37 | 1.24 | −19.29 | 0.93 | 4.42 | 1.78 | −5.53 | 1.48 | (1;1;26) |
| 119 | BX Peg | | | 21 38 49.39 | +26 41 34.20 | 7.10 | 2.50 | −11.90 | 2.50 | 6.13 | 0.77 | 25.00 | 3.00 | (2;5;61) |
| 120 | V445 Cep | 210431 | 109191 | 22 07 10.89 | +72 22 22.26 | 83.91 | 0.51 | 43.90 | 0.42 | 8.95 | 0.50 | 40.69 | 0.95 | (1;1;21) |
| 121 | BB Peg | | 110493 | 22 22 56.89 | +16 19 27.84 | 19.28 | 2.66 | −24.66 | 1.85 | 3.02 | 2.26 | −28.90 | 1.40 | (1;1;11) |
| 122 | V335 Peg | 216417 | 112960 | 22 52 36.18 | +10 13 13.19 | 166.57 | 0.86 | −89.35 | 0.65 | 16.26 | 0.86 | −15.41 | 0.43 | (1;1;21) |
| 123 | SW Lac | 216598 | 113052 | 22 53 41.66 | +37 56 18.61 | 88.16 | 1.25 | 10.79 | 0.82 | 12.30 | 1.26 | −14.46 | 0.90 | (1;1;62) |
| 124 | AB And | | 114508 | 23 11 32.09 | +36 53 35.11 | 109.02 | 1.55 | −53.56 | 0.94 | 8.34 | 1.48 | −27.53 | 0.67 | (1;1;21) |
| 125 | V351 Peg | 220659 | 115627 | 23 25 25.19 | +15 41 19.14 | 17.43 | 0.90 | −16.33 | 0.68 | 7.34 | 0.92 | −8.08 | 0.89 | (1;1;14) |
| 126 | VZ Psc | | 115819 | 23 27 48.39 | +04 51 23.96 | 435.01 | 2.46 | 180.24 | 1.66 | 16.77 | 2.07 | −4.30 | 1.80 | (1;1;63) |
| 127 | BD +14 5016 | | | 23 36 55.37 | +15 48 06.43 | 19.50 | 1.90 | 2.60 | 1.80 | 3.06 | 0.38 | 4.20 | 0.80 | (4;5;64) |
| 128 | EL Aqr | | 117317 | 23 47 18.35 | −08 05 12.09 | −7.23 | 2.53 | 1.00 | 1.65 | 4.71 | 1.89 | 12.51 | 2.08 | (1;1;14) |
| 129 | U Peg | | | 23 57 58.48 | +15 57 10.08 | −46.50 | 1.19 | −53.88 | 0.64 | 7.18 | 1.43 | −28.50 | 1.60 | (1;1;65) |

Therefore, a corresponding 12.5 per cent uncertainty for the photometric parallaxes was taken.

Recent investigations, both visual and spectroscopic, have indicated the presence of additional components for some W UMa binaries. Trigonometric parallaxes are frequently wrong for these systems, as for brighter systems with large uncertainties in the parallaxes. We have preferred not to introduce additional uncertainties into the published data. However, for the reader who wants to estimate the bias introduced by such multiple system, the W UMas with additional components are marked in the last column of Table 5 and are shown by open symbols in the figures.

### 2.2 Radial velocities

All W UMa binaries have circular orbits. Thus, the centre of mass velocity can be obtained simply by fitting a sine curve to the measured radial velocities. However, except for four systems (TW Cet, RZ Tau, TY Pup, AK Her), all W UMa stars in our list had well-determined orbital parameters, so that the centre of mass velocities ($\gamma$) were available with uncertainties. The centre of mass velocities and the associated standard errors are listed in Table 1 with their sources. If there was more than one source available, the data in the latest source were taken because previous radial velocities were used in the later determined orbital parameters. Nevertheless, we have found three systems (V523 Cas, AG Vir, V566 Oph) with multiple orbits which were determined independently from the independent data sets. For these, the weighted mean of the systemic velocities ($\gamma$) and the weighted mean of the associated errors are adopted. Only four systems (TW Cet, RZ Tau, TY Pup, AK Her) had measured centre of mass velocities, but uncertainties were not available. Their uncertainties were estimated from the scatter of component velocities on the radial velocity curve. All different types of errors have been transformed to standard errors for the sake of consistency.

## 3 GALACTIC SPACE AND VELOCITY DISTRIBUTIONS

### 3.1 Sky and space distributions

There is no programme similar to that of the DDO, which contributed 54 per cent of the radial velocities, in the Southern hemisphere, where the number of observatories is already relatively less, so there is a strong bias in the sky distribution of the present W UMa systems. The celestial coordinates ($\alpha$, $\delta$) are plotted in Fig. 1(a) so that the bias is obvious as there are 103 systems (80 per cent) in the Northern hemisphere and 26 systems (20 per cent) in the Southern hemisphere. Unfortunately, the bias is unavoidable because of the following. (i) The present work is established on the accumulated data in the literature and it is not wise to wait for another unknown period without a clue as to how southern systems will be increased. (ii) Eliminating some northern systems to establish isotropy is not

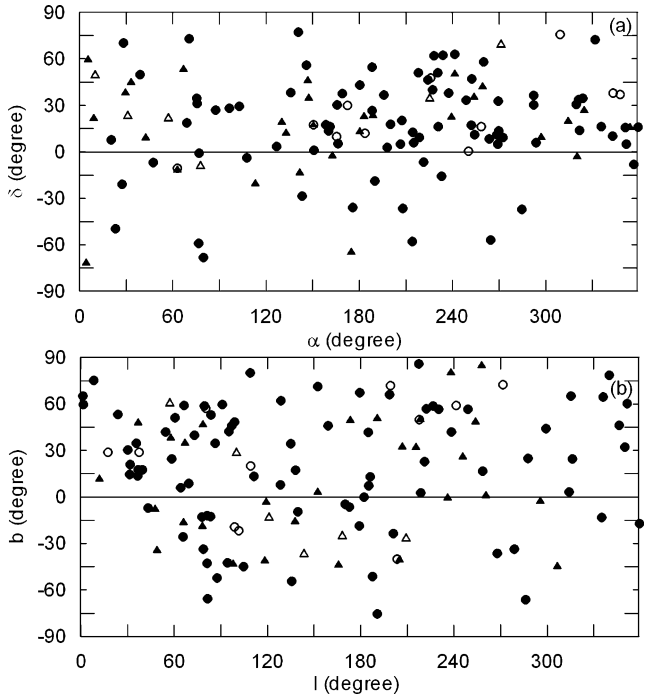


**Figure 1.** Sky distributions of the present sample (a) at the celestial and (b) at the galactic coordinates. Circles denote *Hipparcos* parallaxes, triangles denote that the systems use Rucinski's calibration, filled symbols denote normal W UMa, and open symbols denote W UMas with visible companions.



Downloaded from https://academic.oup.com/mnras/article/357/2/497/1370601 by Akdeniz University user on 20 September 2021

**Table 2.** Kinematic data of the W UMas.

| ID | Name | HD | $l$ (°) | $b$ (°) | $X$(pc) | $Y$(pc) | $Z$(pc) | U (km s$^{-1}$) | | V (km s$^{-1}$) | | W (km s$^{-1}$) | | Code | MG | OC |
|---|---|---|---|---|---|---|---|---|---|---|---|---|---|---|---|---|
| 1 | AQ Tuc | 1372 | 306.66 | −44.97 | 149 | −200 | −249 | −22.76 | 4.77 | −45.28 | 4.28 | −9.93 | 1.43 | | | |
| 2 | BH Cas | | 119.08 | −3.49 | −144 | 259 | −18 | 19.39 | 3.76 | −15.02 | 2.79 | −42.25 | 6.37 | | | |
| 3 | DZ Psc | | 118.30 | −41.20 | −74 | 137 | −136 | 3.73 | 2.42 | −3.05 | 2.69 | 25.60 | 2.71 | | | |
| 4 | V523 Cas | | 121.08 | −12.59 | −41 | 67 | −18 | −43.78 | 5.37 | −35.60 | 4.21 | −28.31 | 3.65 | | | |
| 5 | AQ Psc | 8152 | 135.65 | −54.53 | −52 | 51 | −101 | 4.38 | 0.70 | 3.94 | 1.57 | 14.81 | 0.81 | | | |
| 6 | AE Phe | 9528 | 286.22 | −66.25 | 5 | −19 | −45 | −20.12 | 0.84 | −26.19 | 1.53 | 18.91 | 2.32 | 1, 1 | LA, IC | |
| 7 | TW Cet | | 190.59 | −75.49 | −25 | −5 | −98 | −16.25 | 7.52 | −20.14 | 7.04 | −15.53 | 24.24 | 1, 1, 2 | Cas, IC, LA | |
| 8 | V776 Cas | | 128.21 | 7.81 | −126 | 160 | 28 | −2.16 | 4.33 | −30.62 | 3.90 | 5.20 | 2.95 | | | |
| 9 | QX And | | 11.91 | 11.43 | 365 | 77 | 75 | −24.12 | 3.70 | −16.87 | 4.41 | −17.36 | 4.39 | 1, 1 | LA, IC | NGC 752 |
| 10 | SS Ari | | 143.57 | −35.94 | −138 | 102 | −125 | −16.66 | 2.87 | −24.10 | 3.63 | 0.86 | 2.18 | 1, 1 | IC, LA | |
| 11 | GZ And | | 137.72 | −15.87 | −116 | 105 | −44 | 5.46 | 1.90 | 7.72 | 1.89 | −4.07 | 1.95 | 1 | UMa | |
| 12 | V376 And | 15922 | 139.55 | −9.63 | −148 | 126 | −33 | −51.49 | 5.50 | −18.45 | 5.92 | 7.15 | 2.03 | | | |
| 13 | EE Cet | 17613 | 165.58 | −43.91 | −96 | 25 | −95 | −19.66 | 3.26 | −19.71 | 4.03 | 11.64 | 2.87 | | | |
| 14 | UX Eri | | 187.70 | −51.44 | −94 | −13 | −119 | −15.59 | 3.79 | −14.45 | 6.13 | −2.20 | 3.67 | 1, 1 | IC, LA | |
| 15 | EQ Tau | | 168.13 | −24.65 | −128 | 27 | −60 | −81.50 | 2.42 | −31.50 | 5.71 | −14.52 | 2.48 | | | |
| 16 | BL Eri | | 205.10 | −40.70 | −248 | −116 | −235 | −32.39 | 3.65 | −23.90 | 4.63 | −11.85 | 4.04 | | | |
| 17 | YY Eri | 26609 | 203.50 | −40.04 | −39 | −17 | −36 | 40.04 | 2.22 | 2.37 | 0.57 | −20.96 | 2.28 | | | |
| 18 | AO Cam | | 152.16 | 2.94 | −96 | 51 | 6 | 3.61 | 1.25 | −18.18 | 1.92 | −3.46 | 1.33 | | | |
| 19 | RZ Tau | 285892 | 179.21 | −18.72 | −165 | 2 | −56 | 1.85 | 47.40 | 9.78 | 3.31 | −20.82 | 17.25 | | | |
| 20 | DN Cam | 29213 | 137.97 | 17.30 | −158 | 142 | 66 | −12.77 | 1.22 | 9.48 | 1.34 | −20.48 | 4.48 | 1 | UMa | |
| 21 | V410 Aur | 280332 | 170.06 | −4.65 | −206 | 36 | −17 | −39.23 | 3.88 | −2.64 | 11.36 | 0.87 | 6.13 | | | |
| 22 | V402 Aur | 282719 | 172.79 | −6.45 | −141 | 18 | −16 | −41.93 | 0.96 | −1.58 | 1.56 | −1.78 | 1.09 | | | |
| 23 | AP Dor | 33474 | 267.96 | −36.37 | −6 | −173 | −127 | −82.31 | 17.16 | −30.34 | 5.03 | 33.94 | 7.58 | | | |
| 24 | V1363 Ori | 289949 | 201.09 | −23.44 | −90 | −35 | −42 | −22.53 | 2.85 | −34.53 | 5.65 | −15.88 | 1.27 | | | |
| 25 | ER Ori | | 209.20 | −26.13 | −126 | −70 | −71 | −16.64 | 2.97 | −32.93 | 2.67 | −20.00 | 1.87 | | | |
| 26 | RW Dor | 269320 | 278.77 | −33.62 | 14 | −92 | −62 | −23.25 | 7.63 | −85.23 | 6.89 | 0.64 | 8.40 | | | |
| 27 | V781 Tau | 248087 | 182.21 | −0.15 | −81 | −3 | 0 | −23.71 | 1.30 | −12.75 | 1.37 | −43.84 | 4.83 | | | |
| 28 | AH Aur | 256902 | 185.15 | 7.31 | −160 | −14 | 21 | −29.16 | 1.60 | −16.32 | 4.75 | 10.01 | 2.54 | | | |
| 29 | QW Gem | 264672 | 186.19 | 12.82 | −237 | −26 | 54 | 6.50 | 7.06 | −30.72 | 41.87 | 6.47 | 12.26 | | | |
| 30 | V753 Mon | 54975 | 218.61 | 2.56 | −149 | −119 | 9 | −26.33 | 0.78 | −25.43 | 0.81 | −12.98 | 3.04 | 2 | IC | |
| 31 | TY Pup | 60265 | 236.04 | −0.72 | −120 | −178 | −3 | −51.62 | 17.50 | 4.56 | 25.11 | −1.09 | 1.11 | | | |
| 32 | FG Hya | | 221.03 | 22.83 | −238 | −207 | 133 | 61.63 | 33.93 | −78.64 | 53.82 | −37.89 | 23.38 | | | |
| 33 | TX Cnc | | 206.62 | 32.17 | −145 | −73 | 102 | −42.09 | 3.67 | −22.51 | 3.60 | −24.46 | 5.27 | | | M 44 |
| 34 | AH Cnc | | 215.68 | 31.99 | −574 | −412 | 441 | −6.11 | 7.33 | −35.39 | 9.38 | −28.54 | 9.59 | | | M 67 |
| 35 | UV Lyn | | 184.74 | 41.51 | −91 | −8 | 81 | −27.58 | 5.69 | 12.21 | 2.45 | −30.62 | 6.15 | | | |
| 36 | FN Cam | 79886 | 135.15 | 34.44 | −162 | 161 | 156 | −30.57 | 5.05 | −22.65 | 8.09 | 19.53 | 3.45 | 1 | LA | |
| 37 | EZ Hya | | 245.81 | 25.69 | −68 | −151 | 80 | −20.97 | 3.38 | −14.28 | 1.31 | −11.86 | 3.29 | 1, 2 | LA, IC | |
| 38 | S Ant | 82610 | 258.55 | 16.61 | −14 | −71 | 21 | −30.51 | 1.82 | 8.15 | 1.70 | −12.40 | 0.80 | | | |
| 39 | W UMa | 83950 | 158.92 | 45.90 | −32 | 12 | 36 | 21.01 | 0.82 | −13.19 | 0.45 | −17.29 | 0.91 | | | |



Downloaded from https://academic.oup.com/mnras/article/357/2/497/1370601 by Akdeniz University user on 20 September 2021

**Table 2** – *continued*

| ID | Name | HD | $l$ (°) | $b$ (°) | $X$(pc) | $Y$(pc) | $Z$(pc) | U (km s$^{-1}$) | | V (km s$^{-1}$) | | W (km s$^{-1}$) | | Code | MG | OC |
|---|---|---|---|---|---|---|---|---|---|---|---|---|---|---|---|---|
| 40 | AA UMa | | 173.25 | 49.21 | −203 | 24 | 237 | 20.99 | 3.09 | −9.41 | 3.81 | −26.42 | 2.82 | | | |
| 41 | RT Lmi | | 190.74 | 50.64 | −203 | −38 | 252 | 13.20 | 3.29 | −6.83 | 3.98 | −4.65 | 2.82 | | | |
| 42 | XY Leo | | 217.80 | 49.74 | −32 | −25 | 48 | 45.60 | 2.46 | 6.51 | 1.72 | −32.13 | 1.70 | | | |
| 43 | XZ Leo | | 218.44 | 49.80 | −195 | −155 | 295 | −19.18 | 3.99 | 0.06 | 1.54 | −18.35 | 3.03 | 1, 1 | LA, Cas | |
| 44 | Y Sex | 87079 | 238.49 | 41.94 | −43 | −70 | 74 | −0.95 | 1.88 | −7.13 | 1.58 | 6.14 | 1.87 | | | |
| 45 | ET Leo | 91386 | 222.34 | 56.81 | −29 | −27 | 60 | −17.73 | 1.15 | −13.03 | 0.67 | 10.95 | 1.01 | | | |
| 46 | UZ Leo | | 230.28 | 56.60 | −56 | −68 | 133 | −8.66 | 3.55 | −1.22 | 1.46 | −14.91 | 2.32 | 1 | UMa | |
| 47 | EX Leo | 93077 | 226.62 | 58.85 | −36 | −38 | 87 | 1.33 | 0.77 | −15.00 | 2.24 | −19.42 | 1.49 | | | |
| 48 | VY Sex | 93917 | 253.81 | 48.30 | −25 | −87 | 102 | 15.60 | 2.67 | −56.00 | 5.65 | −21.28 | 4.39 | | | |
| 49 | AM Leo | | 241.50 | 59.02 | −19 | −35 | 66 | 1.26 | 1.62 | −12.59 | 3.08 | −0.05 | 1.87 | 1 | Cas | |
| 50 | VW Lmi | 95660 | 198.56 | 66.04 | −48 | −16 | 114 | 5.48 | 0.98 | −0.49 | 0.42 | 7.51 | 0.80 | 1, 2 | Cas, UMa | |
| 51 | AP Leo | | 249.13 | 56.47 | −24 | −62 | 101 | 67.11 | 12.50 | 2.03 | 2.59 | −13.45 | 2.39 | | | |
| 52 | HN UMa | | 179.28 | 67.35 | −66 | 1 | 159 | 63.15 | 11.73 | −11.70 | 2.90 | −13.80 | 4.94 | | | |
| 53 | AW UMa | 99946 | 199.11 | 71.93 | −19 | −7 | 63 | 7.01 | 0.54 | −65.57 | 4.02 | −22.78 | 1.55 | | | |
| 54 | TV Mus | 310730 | 295.42 | −2.99 | 99 | −209 | −12 | 34.61 | 6.06 | 10.03 | 2.97 | 0.76 | 3.72 | | | |
| 55 | V752 Cen | 101799 | 287.63 | 25.01 | 29 | −91 | 44 | −8.12 | 2.97 | −39.68 | 2.37 | −5.22 | 2.77 | | | |
| 56 | AG Vir | 104350 | 260.60 | 0.72 | −33 | −197 | 3 | 11.70 | 1.43 | −13.09 | 1.99 | −10.20 | 0.94 | | | |
| 57 | HX UMa | 104425 | 152.16 | 71.14 | −43 | 23 | 142 | 51.86 | 21.15 | 4.70 | 3.77 | −5.90 | 5.94 | | | |
| 58 | CC Com | | 238.04 | 79.97 | −7 | −12 | 79 | −41.89 | 5.34 | −13.52 | 2.07 | −16.34 | 1.51 | | | |
| 59 | AH Vir | 106400 | 271.52 | 72.39 | 1 | −28 | 88 | 42.13 | 11.89 | −30.79 | 8.29 | −3.19 | 2.86 | | | Wolf 630 |
| 60 | II UMa | 109247 | 128.65 | 62.13 | −58 | 72 | 175 | −29.02 | 10.65 | −32.09 | 10.61 | −4.69 | 1.45 | 1, 1 | Hya, IC | |
| 61 | RW Com | | 217.61 | 85.87 | −5 | −4 | 87 | −33.71 | 7.99 | −37.02 | 8.48 | −56.70 | 1.41 | | | |
| 62 | RZ Com | | 257.75 | 84.70 | −4 | −19 | 212 | 21.35 | 3.06 | −0.24 | 1.39 | −1.42 | 1.67 | | | Coma |
| 63 | SX Crv | 110139 | 299.25 | 43.99 | 32 | −58 | 64 | 19.62 | 1.76 | 1.69 | 1.06 | 5.01 | 0.72 | | | |
| 64 | BI CVn | | 108.86 | 80.19 | −10 | 30 | 186 | 3.13 | 1.55 | −16.11 | 4.86 | −2.52 | 1.97 | 1 | Cas | |
| 65 | KZ Vir | 114726 | 315.40 | 65.02 | 46 | −45 | 139 | −5.49 | 0.99 | −1.82 | 0.67 | −3.29 | 0.48 | 1, 1 | UMa, Cas | |
| 66 | KR Com | 115955 | 339.81 | 78.52 | 14 | −5 | 75 | 13.68 | 1.03 | −24.99 | 1.71 | −12.35 | 0.49 | | | |
| 67 | HT Vir | 119931 | 335.97 | 64.42 | 26 | −11 | 59 | −32.25 | 4.21 | −19.12 | 4.16 | −15.40 | 1.21 | | | |
| 68 | XY Boo | | 8.30 | 75.08 | 87 | 13 | 329 | −54.47 | 31.71 | 10.42 | 6.48 | 16.05 | 8.36 | | | |
| 69 | V757 Cen | 120734 | 316.25 | 24.68 | 46 | −44 | 29 | 6.12 | 2.73 | −66.49 | 3.15 | 12.13 | 1.28 | | | |
| 70 | RR Cen | 124689 | 314.13 | 3.15 | 71 | −73 | 6 | −28.95 | 1.77 | −8.09 | 1.73 | −2.83 | 0.34 | | | |
| 71 | VW Boo | | 1.29 | 65.15 | 122 | 3 | 264 | 54.78 | 24.84 | −46.53 | 25.75 | 1.43 | 11.26 | | | |
| 72 | NN Vir | 125488 | 351.55 | 60.16 | 52 | −8 | 91 | −16.14 | 1.68 | −24.65 | 3.03 | 0.02 | 0.89 | 1 | Cas | |
| 73 | EF Boo | 234150 | 90.81 | 59.53 | −1 | 85 | 144 | 2.98 | 1.23 | −40.40 | 6.03 | 8.54 | 3.66 | | | |
| 74 | CK Boo | 128141 | 1.46 | 59.62 | 79 | 2 | 135 | 89.49 | 14.89 | −13.67 | 3.02 | −9.34 | 8.71 | | | |
| 75 | GR Vir | 129903 | 346.23 | 46.34 | 36 | −9 | 38 | −65.96 | 1.31 | 6.30 | 0.48 | −36.32 | 1.19 | | | |
| 76 | AC Boo | | 79.26 | 58.76 | 13 | 67 | 113 | −10.53 | 1.55 | −5.11 | 1.32 | −6.05 | 1.94 | 1, 2 | UMa, Cas | |
| 77 | TY Boo | | 57.19 | 61.33 | 45 | 69 | 151 | −60.77 | 6.19 | −32.24 | 2.71 | −15.53 | 3.08 | | | |
| 78 | 44 Boo | 133640 | 80.37 | 57.07 | 1 | 7 | 11 | −17.74 | 0.22 | −26.52 | 0.32 | −2.48 | 0.38 | 1, 1 | LA, IC | |
| 79 | TZ Boo | | 66.21 | 59.00 | 31 | 70 | 127 | −77.39 | 15.00 | −34.97 | 4.05 | −5.34 | 5.93 | | | |

© 2005 RAS, MNRAS **357,** 497–517

Downloaded from https://academic.oup.com/mnras/article/357/2/497/1370601 by Akdeniz University user on 20 September 2021

**Table 2** – *continued*

| ID | Name | HD | $l$ (°) | $b$ (°) | $X$(pc) | $Y$(pc) | $Z$(pc) | U (km s$^{-1}$) | | V (km s$^{-1}$) | | W (km s$^{-1}$) | | Code | MG | OC |
|---|---|---|---|---|---|---|---|---|---|---|---|---|---|---|---|---|
| 80 | BW Dra | | 98.92 | 48.20 | −7 | 43 | 49 | −46.26 | 17.50 | −60.90 | 7.33 | −34.00 | 4.21 | | | |
| 81 | BV Dra | 135421 | 98.92 | 48.20 | −7 | 44 | 50 | −49.41 | 9.44 | −63.77 | 4.19 | −32.77 | 2.56 | | | |
| 82 | FI Boo | 234224 | 83.58 | 52.83 | 7 | 63 | 84 | −33.41 | 6.64 | −20.03 | 1.11 | −20.57 | 1.25 | | | |
| 83 | OU Ser | 136924 | 23.62 | 53.38 | 32 | 14 | 46 | −90.14 | 3.02 | −85.33 | 3.85 | 6.68 | 3.21 | | | |
| 84 | VZ Lib | | 350.03 | 32.15 | 169 | −30 | 108 | −31.88 | 3.54 | −7.19 | 4.97 | −9.09 | 3.66 | | | |
| 85 | FU Dra | | 97.07 | 45.80 | −14 | 111 | 115 | −104.20 | 17.84 | −132.80 | 21.82 | 100.22 | 18.93 | | | |
| 86 | YY CrB | 141990 | 60.49 | 51.14 | 27 | 48 | 69 | −19.64 | 1.34 | −20.46 | 1.48 | 15.69 | 1.66 | 1 | LA | |
| 87 | AU Ser | | 36.85 | 47.84 | 98 | 74 | 136 | −15.35 | 3.18 | −70.45 | 5.81 | −37.06 | 2.17 | | | |
| 88 | V842 Her | | 78.53 | 46.61 | 22 | 111 | 120 | −33.79 | 3.39 | −47.35 | 2.04 | −30.18 | 2.28 | | | |
| 89 | BX Dra | | 95.18 | 42.39 | −20 | 218 | 199 | −18.02 | 4.90 | −24.07 | 3.20 | −13.61 | 2.91 | 2 | LA | |
| 90 | V899 Her | 149684 | 54.48 | 41.85 | 54 | 75 | 83 | 16.82 | 2.58 | −7.59 | 0.89 | −30.70 | 2.08 | | | |
| 91 | V502 Oph | 150484 | 17.22 | 28.85 | 71 | 22 | 41 | −43.03 | 1.01 | −11.85 | 0.55 | −8.35 | 1.39 | | | |
| 92 | V918 Her | 151701 | 35.67 | 34.70 | 77 | 55 | 65 | −26.09 | 0.97 | −12.83 | 0.51 | −5.68 | 1.11 | | | |
| 93 | V921 Her | 152172 | 73.07 | 39.89 | 93 | 307 | 268 | −32.59 | 3.21 | −46.14 | 5.14 | −62.25 | 4.97 | | | |
| 94 | V829 Her | | 57.87 | 37.91 | 31 | 49 | 45 | −2.89 | 0.96 | −13.92 | 1.05 | −5.69 | 1.06 | 1 | Cas | |
| 95 | V2357 Oph | | 30.01 | 30.29 | 139 | 80 | 94 | 41.96 | 21.92 | −70.24 | 23.12 | −43.51 | 12.77 | | | |
| 96 | AK Her | 155937 | 37.51 | 28.73 | 66 | 51 | 46 | 6.27 | 11.35 | −13.70 | 8.24 | −23.09 | 8.52 | | | |
| 97 | V728 Her | | 66.80 | 34.53 | 135 | 314 | 235 | 18.32 | 5.03 | 3.22 | 4.24 | 40.57 | 4.80 | | | |
| 98 | GM Dra | 238677 | 86.44 | 34.70 | 5 | 81 | 56 | 29.12 | 2.72 | 25.10 | 2.05 | −22.99 | 2.65 | | | |
| 99 | V2377 Oph | 159356 | 31.50 | 20.92 | 79 | 48 | 35 | −5.37 | 2.03 | −35.08 | 2.72 | −15.51 | 0.88 | | | |
| 100 | V535 Ara | 159441 | 335.18 | −13.20 | 100 | −46 | −26 | −27.84 | 1.48 | −34.51 | 4.23 | 25.82 | 2.26 | | | |
| 101 | V2388 Oph | 163151 | 36.62 | 17.68 | 52 | 39 | 21 | 13.72 | 1.95 | −60.46 | 2.53 | −9.47 | 0.31 | | | |
| 102 | V566 Oph | 163611 | 31.17 | 14.40 | 59 | 36 | 18 | −51.35 | 1.51 | 5.19 | 2.22 | −15.60 | 0.60 | | | |
| 103 | V972 Her | 164078 | 58.48 | 24.76 | 29 | 48 | 26 | 8.36 | 0.38 | −5.23 | 0.48 | 8.10 | 0.34 | | | |
| 104 | V508 Oph | | 39.37 | 17.66 | 96 | 79 | 40 | −9.74 | 5.59 | −44.05 | 6.25 | −14.24 | 1.52 | | | |
| 105 | EF Dra | | 100.05 | 29.28 | −27 | 150 | 85 | 23.06 | 3.21 | −38.19 | 3.22 | −10.67 | 2.85 | | | |
| 106 | V839 Oph | 166231 | 36.43 | 13.47 | 97 | 71 | 29 | −51.27 | 0.46 | −44.85 | 1.50 | 2.60 | 3.19 | | | |
| 107 | eps Cra | 175813 | 359.54 | −17.32 | 29 | 0 | −9 | 58.62 | 1.15 | −21.94 | 0.60 | −5.98 | 0.51 | | | |
| 108 | V401 Cyg | | 64.13 | 6.00 | 38 | 77 | 9 | 13.96 | 4.34 | 20.41 | 2.85 | 2.04 | 3.37 | | | |
| 109 | V2082 Cyg | 183752 | 69.40 | 8.70 | 32 | 84 | 14 | −52.31 | 1.96 | −19.09 | 0.84 | 5.75 | 0.60 | | | |
| 110 | V417 Aql | | 43.21 | −7.03 | 95 | 89 | −16 | −3.73 | 3.06 | −20.52 | 3.50 | −4.37 | 2.48 | | | |
| 111 | OO Aql | 187183 | 47.82 | −8.17 | 102 | 113 | −22 | −50.97 | 2.41 | −25.70 | 1.39 | −37.60 | 5.46 | | | |
| 112 | VW Cep | 197433 | 109.22 | 20.06 | −9 | 25 | 9 | −74.79 | 2.08 | −34.81 | 1.16 | 0.20 | 0.38 | | | |
| 113 | LS Del | 199497 | 66.00 | −16.49 | 31 | 69 | −22 | −67.49 | 6.78 | −5.48 | 2.45 | −15.62 | 2.89 | | | |
| 114 | V2150 Cyg | 202924 | 77.81 | −13.04 | 43 | 201 | −48 | −5.65 | 1.37 | −14.26 | 0.83 | −3.11 | 2.30 | | | |
| 115 | HV Aqr | | 48.99 | −34.47 | 77 | 89 | −81 | 54.48 | 7.28 | −50.34 | 5.94 | 5.91 | 1.35 | | | |
| 116 | V1073 Cyg | 204038 | 81.13 | −11.95 | 28 | 178 | −38 | 10.46 | 3.45 | −5.33 | 1.43 | −9.53 | 2.73 | | | |
| 117 | KP Peg | 204215 | 65.75 | −25.73 | 85 | 188 | −99 | 5.53 | 3 .88 | −2.13 | 2.72 | −7.30 | 2.74 | 1, 2 | Cas, UMa | |
| 118 | DK Cyg | | 83.29 | −12.76 | 26 | 219 | −50 | 29.62 | 14.63 | −8.34 | 1.87 | 7.08 | 2.64 | | | |
| 119 | BX Peg | | 78.21 | −19.00 | 32 | 151 | −53 | 2.52 | 2.00 | 19.22 | 2.91 | −17.99 | 2.40 | | | |



Downloaded from https://academic.oup.com/mnras/article/357/2/497/1370601 by Akdeniz University user on 20 September 2021

**Table 2** – *continued*

| ID | Name | HD | $l$ (°) | $b$ (°) | $X$(pc) | $Y$(pc) | $Z$(pc) | U (km s$^{-1}$) | V (km s$^{-1}$) | W (km s$^{-1}$) | Code | MG | OC |
|---|---|---|---|---|---|---|---|---|---|---|---|---|---|
| 120 | V445 Cep | 210431 | 111.13 | 13.38 | −39 | 101 | 26 | −63.88 | 20.92 | 1.51 | 0.55 | | |
| 121 | BB Peg | | 78.90 | −33.56 | 53 | 271 | −183 | −15.44 | −50.75 | −24.94 | 30.77 | | |
| 122 | V335 Peg | 216417 | 81.25 | −42.83 | 7 | 45 | −42 | −30.97 | −41.28 | −26.21 | 1.97 | 1 | Hya |
| 123 | SW Lac | 216598 | 98.68 | −19.33 | −12 | 76 | −27 | −31.07 | −22.24 | −6.60 | 1.25 | 1, 1 | LA, IC |
| 124 | AB And | | 101.60 | −21.81 | −22 | 109 | −45 | −37.31 | −53.16 | −38.91 | 8.74 | | |
| 125 | V351 Peg | 220659 | 94.40 | −42.37 | −8 | 100 | −92 | −6.95 | −16.05 | −5.22 | 1.51 | 1 | IC |
| 126 | VZ Psc | | 87.50 | −52.17 | 2 | 37 | −47 | −133.25 | −12.75 | −8.92 | 2.11 | | |
| 127 | BD +14 5016 | | 97.90 | −43.42 | −33 | 235 | −225 | −35.15 | −6.46 | −8.78 | 2.24 | 1 | LA |
| 128 | EL Aqr | | 81.40 | −65.65 | 13 | 87 | −193 | 4.31 | 8.92 | −9.27 | 2.24 | | |
| 129 | U Peg | | 104.61 | −45.01 | −25 | 95 | −99 | 45.41 | −26.60 | 2.41 | 3.73 | | |

feasible because it would greatly reduce the statistical significance of the sample. Due to the angle (63°) between the celestial equator and the galactic plane, the distribution of the sample in galactic coordinates (Fig. 1b) appears to be less affected by the bias. Nevertheless, this is only an illusion because un-isotropy would not change by changing the coordinate system.

In order to inspect the space distributions of the present W UMa sample, the Sun centred rectangular galactic coordinates ($X$ towards the Galactic Centre, $Y$ Galactic rotation, $Z$ North Galactic Pole) were calculated. The ($X$, $Y$, $Z$) space coordinates are given in Table 2. The projected positions on the Galactic plane ($X$, $Y$ plane) and on the plane perpendicular to it ($X$, $Z$ plane) are displayed in Fig. 2. The bias on the prime reference frames ($X$–$Y$, $X$–$Z$ and $Y$–$Z$) are not as obvious as in Fig. 1(a). Having 69 systems with $X < 0$ and 60 systems with $X > 0$, the $Y$–$Z$ plane shows the least bias. Having 65 and 44 systems the northern and southern Galactic latitudes, the Galactic plane ($X$–$Y$) shows the strongest bias (Fig. 2) but still it is not as obvious as in Fig. 1(a).

With a median distance of 137 pc, the sample contains relatively nearby systems and it can be considered within the Galactic thin disc. Occupying almost the same space in the solar neighbourhood, the CAB sample (Karataş et al. 2004) has a smaller median distance (98 pc) than the W UMa sample. Thus, we were curious to compare the space dispersions of the present W UMa sample and the CAB sample. In order to avoid the complications of far distant members, the space dispersions of both samples within 300 pc are calculated. Indeed, with the space dispersions of $\delta X = \pm 78$ pc, $\delta Y = \pm 90$ pc and $\delta Z = \pm 87$ pc, the W UMa sample seems slightly more dispersed than the CAB sample with the space dispersions of $\delta X = \pm 77$ pc, $\delta Y = \pm 75$ pc and $\delta Z = \pm 73$ pc.

Considering the fact that CABs are, on average, brighter than the less common W UMas, we expected the opposite, because CABs would be visible at longer distances. Obviously, the observational selection is more affected by the easy recognition of W UMas rather than the higher absolute brightness of CABs. Apparently, less bright contact binaries were identified and studied more than CABs at similar distances.

### 3.2 Galactic space velocities

Galactic space velocity components ($U$, $V$, $W$) were computed by applying the algorithm and the transformation matrices of Johnson & Soderblom (1987) to the basic data: celestial coordinates ($\alpha$, $\delta$), proper motion components ($\mu_\alpha$, $\mu_\delta$), radial velocity ($\gamma$) and the parallax ($\pi$) of each star in Table 1, where the epoch of J2000 coordinates was adopted, as described in the ICRS of the *Hipparcos* and the Tycho Catalogues. The transformation matrices use the notation of the right-handed system. Therefore, $U$, $V$ and $W$ are the components of a velocity vector of a star with respect to the Sun, where $U$ is directed toward the Galactic Centre ($l = 0°$, $b = 0°$), $V$ is in the direction of galactic rotation ($l = 90°$, $b = 0°$) and $W$ is towards the North Galactic Pole ($b = 90°$).

Uncertainties of ($U$, $V$, $W$) space velocity components have been computed by propagating the uncertainties of the input data (proper motions, parallax and radial velocity) by the algorithm also by Johnson & Soderblom (1987). The arithmetic means of the uncertainties for ($U$, $V$, $W$) are $\delta U = \pm 5.52$ km s$^{-1}$, $\delta V = \pm 4.67$ km s$^{-1}$ and $\delta W = \pm 3.75$ km s$^{-1}$. By inspecting the individual errors of space velocity vectors ($S = \sqrt{U^2 + V^2 + W^2}$), we have found only 11 (8.5 per cent) systems with errors larger than $\pm 20$ km s$^{-1}$. If these systems were removed from the sample, the averages would reduce to $\delta U = \pm 4.04$ km s$^{-1}$, $\delta V = \pm 3.12$ km s$^{-1}$ and



Downloaded from https://academic.oup.com/mnras/article/357/2/497/1370601 by Akdeniz University user on 20 September 2021

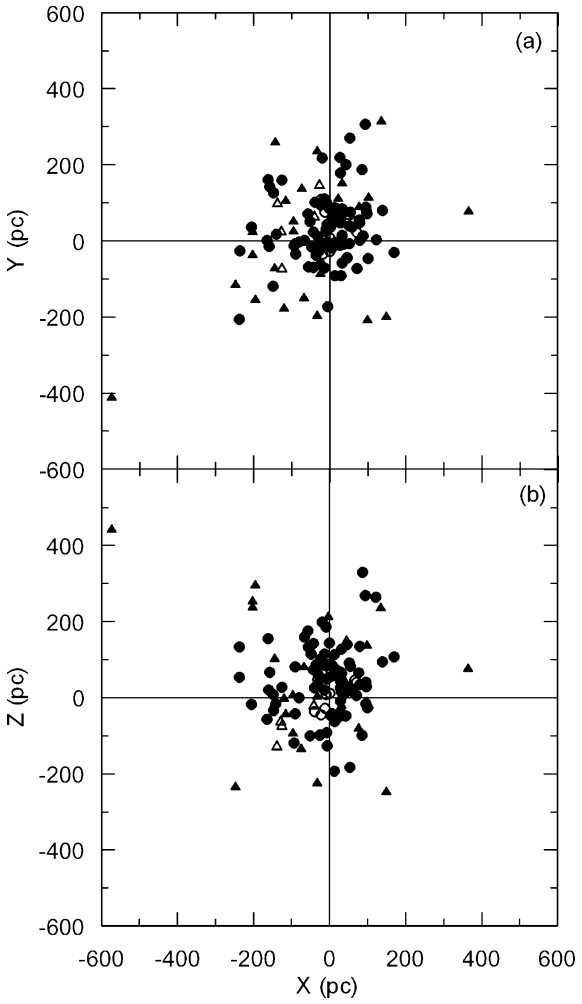


**Figure 2.** The space distributions with respect to the Sun. $X$, $Y$ and $Z$ are heliocentric galactic coordinates directed towards the Galactic Centre, Galactic rotation and the North Galactic Pole. The symbols mean the same as in Fig. 1.

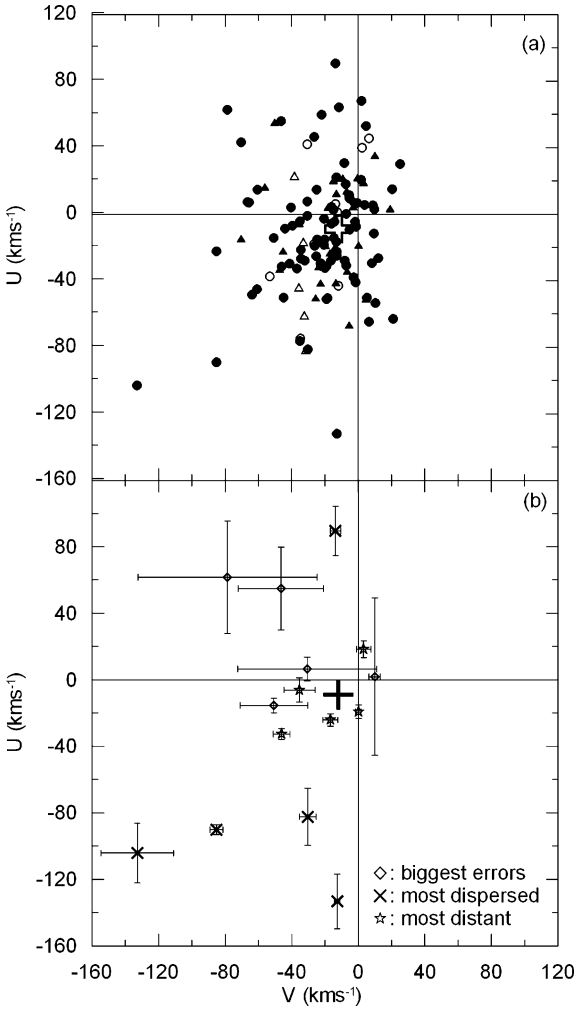


**Figure 3.** (a) Velocity dispersions on the $U$–$V$ plane. (b) Propagated errors of some selected systems. Symbols in (a) are the same as in Fig. 1 and symbols in (b) are self-indicated. The velocities are heliocentric. The position of the LSR is marked by a cross.

$\delta W = \pm 2.68$ km s$^{-1}$. Thus, it can be claimed confidently that most of the sample stars have velocity uncertainties smaller than the velocity dispersions calculated. However, in comparison with the CAB sample (Karataş et al. 2004), the average uncertainties of the present W UMa sample appear nearly two times bigger. Obviously, this is the result of the lower accuracy of W UMa radial velocities because of shorter orbital periods and higher rotation rates.

Having relatively less accurate space velocities, we were curious to check the effect of the differential Galactic rotation. Thus, the first-order Galactic differential rotation contributions to the $U$ and $V$ components were computed as described in Mihalas & Binney (1981). The $W$ velocities are not affected in this first-order approximation. We have found 27 stars (21 per cent) with the contribution from the Galactic differential rotation being greater than the uncertainty of the $U$ component of the space velocity. The effect on the $V$ component is rather small, so that the effect of Galactic differential rotation was found to be smaller than the uncertainties in $V$. Nevertheless, the Galactic differential rotation correction was applied to all of the stars in the present sample. The corrected $U$, $V$ and $W$ are given in Table 2, together with the propagated standard errors.

There is no direct way to estimate how the un-isotropic sky distribution (bias shown in Fig. 1a) affects the W UMa space velocities. However, because the present sample contains only nearby systems within the Galactic thin disc and because first-order Galactic differential rotation correction was applied, the bias seems to be minimized, perhaps removed, in the space velocity distribution. This is because the velocity distribution of the present W UMa sample has a great resemblance to the velocity distribution of the CAB sample (Karataş et al. 2004), which was considered homogeneously and isotropically distributed in the solar neighbourhood. Distribution of the space velocity components on the $U$–$V$ plane is displayed in Fig. 3(a).

In order to display the reliability of computed $U$, $V$ and $W$ velocities, Fig. 3(b) shows the error bars of some selected systems: (i) the five systems that are the most distant; (ii) the five systems with the biggest space velocity vector ($S$); (iii) the five systems that are the most dispersed on the $U$–$V$ diagram. It is also clear in Fig. 3(b) that the propagated uncertainties, even in the extreme cases above, appear smaller than the dispersion, and thus the space velocities ($U$, $V$, $W$) and their dispersions can be considered reliable. Nevertheless, in order to minimize the contribution of the space velocity errors, the dispersions were calculated with respect to the local standard of rest (LSR) rather than arithmetic mean of the space

Downloaded from https://academic.oup.com/mnras/article/357/2/497/1370601 by Akdeniz University user on 20 September 2021

velocities. The position of the LSR is obtained by subtracting the Sun's velocity $(U, V, W)_{\odot} = (9, 12, 7)$ km s$^{-1}$ (Mihalas & Binney 1981) from the frame of $(U, V, W)$ velocities.

### 3.3 Population analysis

As in the CAB sample (Karataş et al. 2004), we have used the parameter $f_{\rm K} = (1/300)(1.0u^2 + 2.5v^2 + 3.5w^2)^{1/2}$ to determine the possible metal-poor binaries kinematically, as suggested by Grenon (1987) and Bartkevicius, Lazauskaite & Bartasiute (1999). Here, the $u$, $v$ and $w$ velocities represent space velocity components with respect to the LSR. Statistically, the stars with $f_{\rm K} \leqslant 0.35$ belong to the thin disc, the stars with $0.35 < f_{\rm K} \leqslant 1.00$ belong to the thick disc, and the stars with $f_{\rm K} > 1$ belong to the halo population.

According to the $f_{\rm K}$ analysis, the vast majority (93 per cent) of our sample are thin disc stars. The possible thick disc members are found to be 7 per cent in the current sample. The thick disc candidates are FU Dra, AP Dor, RW Dor, FG Hya, OU Ser, AU Ser, V921 Her, V2357 Oph and VZ Psc. Spectroscopic metal abundances of W UMa stars appear not to be achievable due to fast rotation and blendings in their spectra. Photometric indices are also entirely unreliable due to the elevated magnetic activity of the W UMa systems. Nevertheless, the photometric metal abundance of BW Dra has been determined by Marsakov & Shevelev (1995) ($[m/H] = -0.56$ dex) and recently by Nordström et al. (2004) ($[m/H] = -0.69$ dex) from the observations of Strömgren photometry. An age of 10.33 Gyr is estimated for it by Marsakov & Shevelev (1995) according to the revised Yale isochrones ages (Green, Demarque & King 1987). If these metal abundances and isochrone ages are correct, with the $f_{\rm K}$ kinematic value of 0.33, BW Dra appears as a star which belongs to the thick disc population although its $f_{\rm K}$ value is slightly less than the lower limit.

Karataş et al. (2004) have found that 7 per cent of CAB binaries are possible members of the thick disc population. It is indeed interesting that the same percentage of thick disc W UMa binaries confirmed in this study coincides with nearly the same ratio, 6 per cent, of solar neighbourhood stars in general belonging to the thick disc population, which were found by Buser, Rong & Karaali (1999), Siegel et al. (2002) and Karaali, Bilir & Hamzaoğlu (2004).

## 4 DISCUSSION

### 4.1 Kinematics of contact binaries

Having only the main-sequence components from the spectral types A to K, the present sample of W UMa binaries appears less heterogeneous than the CAB binaries with the components F to M spectral types of all combinations of the luminosity classes from V to II. Having orbital periods from 1 d to several hundred days, the CAB sample is also considered heterogeneous (Karataş et al. 2004) regarding the period ranges because different orbital periods may represent different evolutionary paths (Plavec 1968; Thomas 1977). However, with a very limited range of short orbital periods ($0.22 < P < 1.13$ d), the W UMa sample can be claimed to be homogeneous, in the sense that all binaries with main-sequence components are in the contact stage. However, the velocity distribution of the W UMa sample on the $U$–$V$ plane (Fig. 2) appears heterogeneous, like the CAB sample, i.e. kinematically younger and older subsystems occupy the same velocity space. With dispersions of 36.5, 26.2 and 19.5 km s$^{-1}$ at $U$, $V$ and $W$ velocity components, it is possible to assign a 4.43-Gyr kinematical age to the whole sample according to the kinematical tables of Wielen (1982). Karataş et al. (2004) assigned an age of 3.86 Gyr to the field CAB binaries. Thus, even before selecting out possible moving group (MG) members, which indeed seem to exist from the appearance of Fig. 3, the W UMa sample is slightly older than the CAB sample.

Guinan & Bradstreet (1988) investigated whether correlations exist between the space velocities and the physical properties of the W UMa systems, such as orbital period ($P$), mass ratio ($q$), system type (A or W), filling factor ($f$), ultraviolet excess and metallicity index. A weak correlation appears possible, in the sense that the space velocities tend to increase with decreasing orbital period. Also, a weak correlation appears, as binaries with large $f$ (overcontact) tend to have higher space velocities. However, no correlation has been found between the space velocities and the mass ratio, the space velocities and the binary type (A or W), and the space velocities and the metallicity index.

In order to search kinematically different subgroups, here we preferred to divide the whole sample into two subsamples according to a criterion, then to compare their $U$–$V$ diagrams. The preliminary criteria and the $U$–$V$ diagrams are summarized and displayed in Fig. 4.

W UMa binaries with spectral types later than F7 tend to have larger dispersions (Figs 4a and b) than W UMas of earlier spectral types. This could be explained by the fact that the later spectral types on the Hertzsprung–Russell (HR) diagram contain older systems because evolution into the main sequence and the duration on the main sequence are longer. However, it is indeed extraordinary that kinematically young and old systems (small and large dispersions) may well exist in both groups. Thus, this criterion fails to provide kinematically homogeneous subsamples.

W UMa stars are classified into A- or W-type systems from their light curves and radial velocity curve (Binnendijk 1970). The W-type systems are those such as W UMa itself, in which the hotter component (the star eclipsed at the primary minimum) is smaller and less massive. Comparison of the $U$–$V$ diagram between the A- and W-type in Fig. 4 confirms Guinan & Bradstreet (1988), in that both groups are indistinguishable kinematically, and that younger and older systems are equally likely to exist in both subgroups of A or W.

If a few high dispersion binaries are removed from the small mass ratio systems, then both subgroups (Figs 4e and f) of the mass ratio criterion will be indistinguishable kinematically. Like the two criteria before, the mass ratio criterion also fails to distinguish younger and older systems homogeneously.

The degree of overfilling ($f$) of the inner critical equipotential surface is an important parameter, which may indicate a stage of an evolution for a contact binary that would coalesce into a single star. FK Com is believed by some to be the product of binary star coalescence (Bopp & Rucinski 1981; Bopp & Stencel 1981). The value of overfilling factor $f$, which depends on how it is defined, changes from minimum, when the system is just in contact, to maximum when components fill out their outer critical envelopes. Different authors define $f$ differently, e.g. Guinan & Bradstreet (1988) define $f$ as $1 \leqslant f \leqslant 2$, but Maceroni & van't Veer (1996) define $f$ as $0 \leqslant f \leqslant 1$. Using the same definition as Maceroni & van't Veer (1996), we have found 109 systems with ($f$). The systems with smaller $f$ are compared to the systems with large $f$ on the $U$–$V$ diagram (Figs 4g and h). The systems with larger $f$ values seem to have larger dispersions, so they appear kinematically older than the systems with smaller $f$. Although this is a natural consequence of the theory of coalescence into a single star, and it may appear to confirm Guinan & Bradstreet (1988), with a careful look at the $U$–$V$ diagrams (Figs 4g and h) one may notice that the two subgroups are not really



Downloaded from https://academic.oup.com/mnras/article/357/2/497/1370601 by Akdeniz University user on 20 September 2021

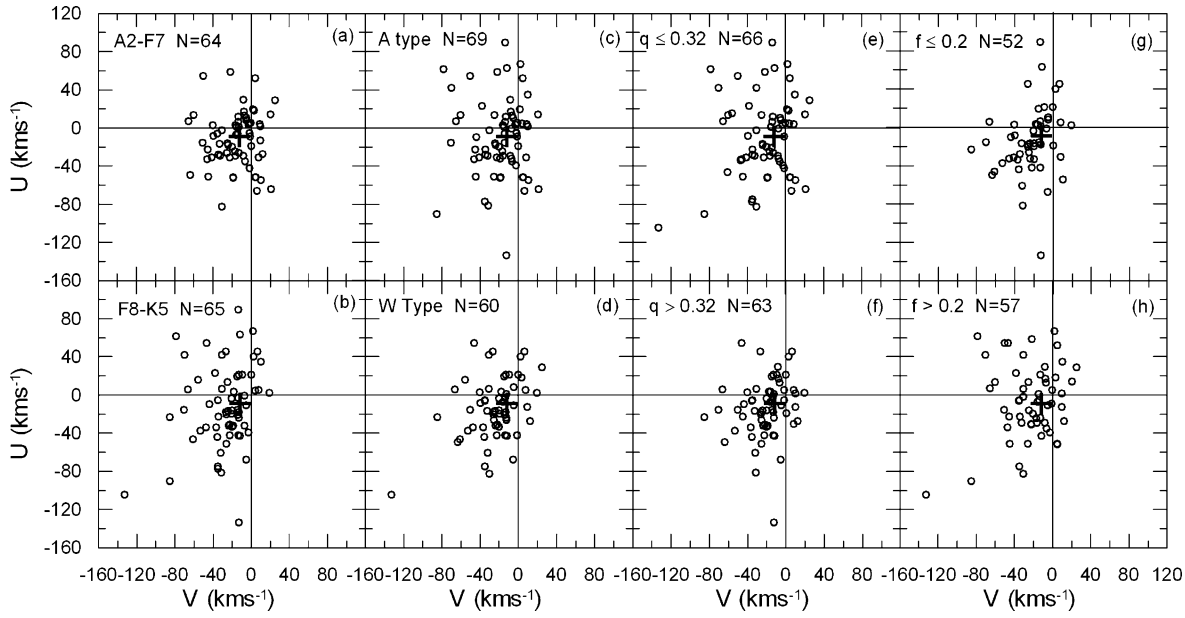


**Figure 4.** Comparison of the space velocity dispersions of various subgroups on the *U–V* diagram: (a) earlier spectral types A2 to F7; (b) later spectral types F8 to K5; (c) A type; (d) W type; (e) mass ratio $q \leqslant 0.32$; (f) mass ratio $q > 0.32$; (g) overcontact parameter $f \leqslant 0.2$; (h) overcontact parameter $f > 0.2$.

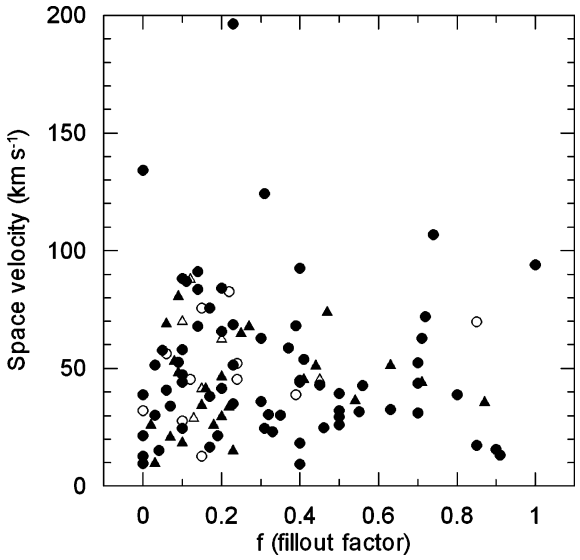


**Figure 5.** The space velocity is plotted against the fill-out factor ($f$) for W UMa binaries.

homogeneous. Kinematically older and younger systems appear to exist in both groups.

In order to make a direct comparison to fig. 9 of Guinan & Bradstreet (1988), the space velocities ($s = \sqrt{u^2 + v^2 + w^2}$) in our sample are plotted against the $f$ values in Fig. 5. According to this presentation, high-velocity stars may well exist at low or high values of $f$. Thus, it can be concluded that the $f$ criterion, like the criteria before (spectral type, binary type (A or W), mass ratio), is not a good criterion to differentiate kinematically older and younger W UMa binaries.

However, this result is consistent with the very brief lifetime of a contact stage, which was predicted by Guinan & Bradstreet (1988) as $0.1 < t_{\rm contact} < 1$ Gyr, and the kinematical age of the sample as a whole, which is 4.43 Gyr. The dispersions in the *U–V* diagram are produced in a time-scale not only covering the contact stage but also covering the pre-contact stages of all. Obviously, the contact stage for many W UMa stars is too short to be effective on the observed dispersions. Therefore, it is possible that a W UMa system with a longer pre-contact evolution may reach a contact configuration at a kinematically larger age such that the $f$ value can be very small. However, on the other hand it is also possible for a W UMa system, with a much shorter pre-contact stage (small kinematical ages), to have a larger value for the $f$. Therefore, the $f$ value criterion fails to discriminate between kinematically young and old systems.

The present W UMa sample was said above to be homogeneous in a narrow range ($0.22 < P < 1.13$ d) of short orbital periods. However, the correlations of orbital periods with the dispersions in the *U–V* diagram are well presented in Fig. 6 in the sense that the short-period W UMa systems have larger dispersions. The subgroups according to the total masses ($M = M_1 + M_2$) display a similar correlation, i.e. less massive systems have larger dispersions than more massive systems.

All subgroups discussed above are summarized numerically in Table 3. The numerical values (velocity averages and dispersions) of the subgroups confirm eye inspection of the dispersions in the *U–V* diagrams of Figs 4 and 6. Indeed, the grouping according to spectral type, system type (A or W), mass ratio and $f$ value in Fig. 4 does not show very many differences in the dispersions. However, grouping according to orbital period and total mass (Fig. 6) is confirmed strongly in Table 3. Using the tables of Wielen (1982), a kinematical age was assigned to each hypothetical subgroup. The ages represent a mean kinematical age of all the stars in a group. The age to be meaningful depends on the how meaningful the group is. The subgroups using orbital period and total mass criteria are indeed meaningful because the decrease of orbital period and total mass, which is established for CABs (Karataş et al. 2004), appears to be a process continuing also in the contact stage. Because of a relatively very short contact stage, there is no guarantee of the subgroups of total mass and orbital period being homogeneous. One way of selecting out younger population W UMa binaries, among the subsamples according to orbital period, is to pick out



Downloaded from https://academic.oup.com/mnras/article/357/2/497/1370601 by Akdeniz University user on 20 September 2021

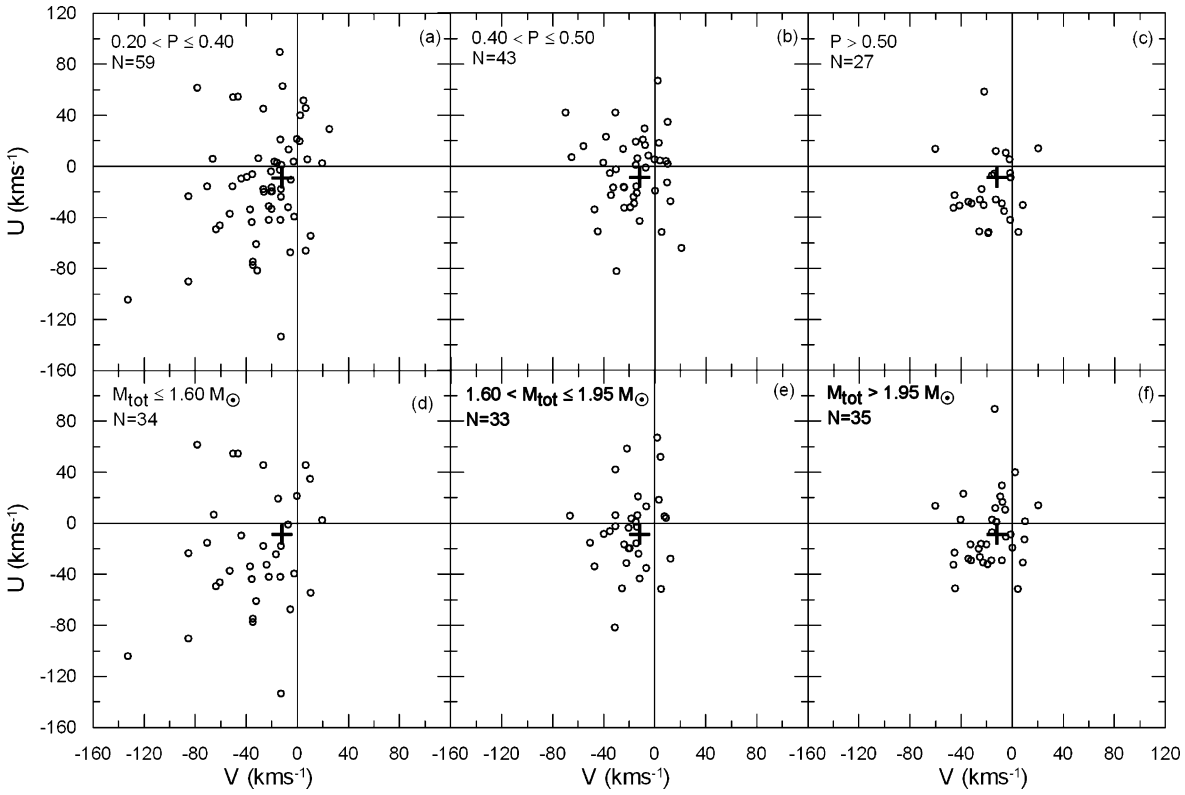


**Figure 6.** Comparison of the space velocity dispersions of period and total mass subgroups on the $U$–$V$ diagram: (a) $0.2 < P \leqslant 0.4$ d; (b) $0.4 < P \leqslant 0.5$ d; (c) $P > 0.5$ d; (d) $M_{\rm tot} \leqslant 1.60$ M$_\odot$; (e) $1.60 < M_{\rm tot} \leqslant 1.95$ M$_\odot$; (f) $M_{\rm tot} > 1.95$ M$_\odot$.

**Table 3.** Kinematical data and the predicted kinematical ages of the subgroups of W UMa.

| Data | N | $\langle U \rangle$ (km s$^{-1}$) | | $\langle V \rangle$ (km s$^{-1}$) | | $\langle W \rangle$ (km s$^{-1}$) | | $\sigma_U$ (km s$^{-1}$) | | $\sigma_V$ (km s$^{-1}$) | | $\sigma_W$ (km s$^{-1}$) | | $\sigma_{\rm tot}$ (km s$^{-1}$) | Age (Gyr) |
|---|---|---|---|---|---|---|---|---|---|---|---|---|---|---|---|
| All | 129 | −12.11 | 0.62 | −21.19 | 0.62 | −8.52 | 0.41 | 36.50 | 7.06 | 26.23 | 7.09 | 19.46 | 4.65 | 49.0 11.0 | 4.43 |
| A2–F7 spectral type | 64 | −12.28 | 0.96 | −15.22 | 0.51 | −6.16 | 0.55 | 28.94 | 7.68 | 21.34 | 4.11 | 17.22 | 4.43 | 39.9 9.8 | 2.83 |
| F8–K5 spectral type | 65 | −11.93 | 0.80 | −27.07 | 1.12 | −10.85 | 0.60 | 42.98 | 6.42 | 30.55 | 9.07 | 21.46 | 4.86 | 56.9 12.1 | 5.88 |
| A type | 69 | −10.55 | 1.02 | −18.40 | 0.88 | −7.85 | 0.45 | 39.86 | 8.51 | 24.17 | 7.31 | 15.93 | 3.77 | 49.3 11.8 | 4.48 |
| W type | 60 | −13.90 | 0.62 | −24.40 | 0.89 | −9.29 | 0.71 | 32.21 | 4.80 | 28.41 | 6.89 | 22.85 | 5.48 | 48.7 10.0 | 4.37 |
| $q \leqslant 0.32$ | 66 | −10.92 | 0.90 | −21.58 | 0.96 | −3.74 | 0.49 | 40.97 | 7.29 | 29.33 | 7.77 | 22.08 | 3.96 | 55.0 11.6 | 5.53 |
| $q > 0.32$ | 63 | −13.34 | 0.86 | −20.78 | 0.80 | −13.54 | 0.67 | 31.15 | 6.80 | 22.52 | 6.34 | 16.26 | 5.30 | 41.7 10.7 | 3.14 |
| $f \leqslant 0.2$ | 52 | −14.06 | 0.73 | −23.16 | 0.31 | −12.24 | 0.48 | 36.41 | 5.30 | 24.36 | 2.22 | 18.70 | 3.48 | 47.6 6.7 | 4.18 |
| $f > 0.2$ | 57 | −7.10 | 1.24 | −23.33 | 1.41 | −6.43 | 0.82 | 38.17 | 8.93 | 30.32 | 10.15 | 21.87 | 5.91 | 53.4 14.7 | 5.24 |
| $0.2 < P \leqslant 0.4$ | 59 | −14.02 | 0.95 | −25.82 | 1.22 | −8.57 | 0.79 | 44.00 | 7.33 | 31.64 | 9.37 | 22.15 | 6.06 | 58.6 13.6 | 6.18 |
| $0.4 < P \leqslant 0.5$ | 43 | −5.46 | 1.23 | −17.29 | 0.55 | −8.96 | 0.49 | 29.72 | 8.09 | 21.66 | 3.59 | 17.36 | 3.24 | 40.7 9.4 | 2.96 |
| $P > 0.5$ | 27 | −18.51 | 0.68 | −17.29 | 0.95 | −7.72 | 0.26 | 26.99 | 3.55 | 18.74 | 4.93 | 16.00 | 1.33 | 36.6 6.2 | 2.30 |
| $M_{\rm tot} \leqslant 1.60$ | 34 | −23.26 | 1.44 | −33.87 | 1.70 | −10.65 | 0.85 | 48.89 | 8.39 | 39.28 | 9.89 | 26.28 | 4.95 | 68.0 13.9 | 7.87 |
| $1.60 < M_{\rm tot} \leqslant 1.95$ | 33 | −5.52 | 0.75 | −18.19 | 1.32 | −8.61 | 0.95 | 31.62 | 4.31 | 18.86 | 7.61 | 16.36 | 5.48 | 40.3 10.3 | 2.90 |
| $1.95 > M_{\rm tot}$ | 35 | −6.89 | 1.43 | −16.89 | 0.73 | −7.95 | 0.79 | 27.59 | 8.46 | 19.01 | 4.31 | 15.78 | 4.65 | 37.0 10.6 | 2.38 |
| MG | 27 | −14.44 | 0.45 | −14.71 | 0.49 | −4.83 | 0.84 | 13.08 | 2.34 | 12.52 | 2.53 | 11.02 | 4.37 | 21.2 5.6 | 0.50 |
| FCB | 97 | −11.99 | 0.80 | −23.00 | 0.81 | −9.22 | 0.49 | 40.92 | 7.86 | 29.31 | 7.97 | 21.45 | 4.80 | 54.7 12.2 | 5.47 |



Downloaded from https://academic.oup.com/mnras/article/357/2/497/1370601 by Akdeniz University user on 20 September 2021

possible MG members, as done in the CAB sample by Karataş et al. (2004).

### 4.2 Possible moving group members among W UMa systems

MGs are kinematically coherent groups of stars that share a common origin. Eggen (1994) defined a supercluster of stars gravitationally unbound in the solar neighbourhood, but sharing the same kinematics while occupying the extended regions in the Galaxy. Therefore, a MG, unlike the well-known open clusters covering a limited region, can be observed all over the sky. The kinematical criteria, which were originally defined by Eggen (1958a,b, 1989, 1995), for determining the possible members of the best-documented MGs are summarized by Montes et al. (2001a,b). Evidence has been found that many young and active late-type binaries can be members of some young MGs (Jeffries 1995; Montes et al. 2001b; King et al. 2003). Indeed, possible MG members determined by Eggen's kinematical criteria have been proved to be very useful for separating the kinematically heterogeneous CAB sample into two subsamples representing younger and older populations (Karataş et al. 2004), which is better than the classical approach of predetermined subgroups with a dividing line of a chosen parameter.

The difficulty of separating kinematically young and old populations in the velocity space is obvious. The dispersions increase with age but there are always some stars naturally occupying the regions near the LSR. It is therefore not safe to pick stars randomly near the LSR and then to form a kinematically young group with them. However, Eggen's kinematical criteria objectively select some stars which have a space velocity vector parallel to the converging point of each predetermined and well-known MG within an acceptable uncertainty. There are two criteria: one sets a range of the direction of the test star's proper motion and the other puts limits on the test star's radial velocity vector. Fulfilling one of the criteria makes the test star a possible member. However, fulfilling both criteria does not guarantee membership, because there is always the possibility that the same velocity space could be occupied by the MG members and the non-members. Further independent criteria implying a common origin and the same age as the member stars are needed to confirm the true membership. Therefore, we should always remember that Eggen's criteria determine only the possible members of an MG. The parameters of the five best-documented MGs and the possible membership criteria for them have been summarized by Karataş et al. (2004) for CABs. Here we apply the same criteria to the stars in the present W UMa sample, and 28 systems were found to satisfy at least one of the criteria for one of the five MGs listed in Table 4. The possible MG members among the W UMa binaries in the present sample are marked in column 16 of Table 2 with the names of the associated MG.

After determining the possible MGs, the whole sample has been divided into three subgroups. The first contains the possible MG members and named MG. The second group contains only five stars, previously known to be the members of well-known open clusters. The third group is the 'field contact binary' (FCB) group, which contains field W UMa systems free from the possible MG and the known open cluster members in the solar neighbourhood. Fig. 7 compares the $U$–$V$ diagram of the MG and FCB group. The detailed kinematics and implied kinematical ages of the MG and FCB group are included in Table 3.

The velocity dispersions of FCBs imply a mean kinematical age of 5.47 Gyr. The mean kinematical age is found to be 500 Myr for the possible MG members. Although this age appears to be consistent with the ages of the MG in Table 4, it may not represent the true mean kinematical ages of all possible MG members. This is because the ages in Table 3 are estimated from the dispersions with respect to the LSR. In reality, each MG has its own centre of dispersion, which is slightly different from the LSR. Therefore, we should keep in mind that members should be at the age of each MG listed in Table 4.

### 4.3 Comparing physical parameters between the field contact binary group and the moving group

The kinematical criteria select out kinematically young W UMa systems without a dividing line according to any physical parameter of W UMa characteristics. However, this does not mean that all kinematically young W UMas are removed from the main sample when forming the MG. There could be systems as young as the MG in the FCB group. These are the systems which fail to satisfy kinematical criteria although they are young. Therefore, all sorts of W UMa systems, young and old, may exist in the FCB group. Thus, the 5.47-Gyr kinematical age represents an average age of all stars in the FCB group. On the other hand, we must remember that the MG stars are not young because of their small dispersions on the velocity space. On the contrary, their dispersions are small because they are young. They are young primarily because they are possible members of the young MGs in Table 4. Nevertheless, the word 'possible' implies that a limited number of non-members may well exist in the MG, which we believe does not change the statistic of the young W UMa phenomenon.

Comparing the MG group and field CABs, Karataş et al. (2004) found some important clues indicating mass loss and orbital period

**Table 4.** The parameters of the best-documented MGs. Column 4 gives the space velocity vector of the MG as a whole ($V_T = \sqrt{U^2 + V^2 + W^2}$). Column 5 gives the direction of the space velocity vector (C. P. represents the converging point in celestial coordinates).

| Name | Age (Myr) | ($U$, $V$, $W$) (km s$^{-1}$) | $V_T$ (km s$^{-1}$) | C. P. ($\alpha^h$, $\delta^\circ$) |
|---|---|---|---|---|
| Local Association (Pleiades, $\alpha$ Per, M34, $\delta$Lyr, NGC 2516, IC 2602) | 20–150 | (−11.6,−21.0,−11.4) | 26.5 | (5.98,−35.15) |
| IC 2391 Supercluster (IC 2391) | 35–55 | (−20.6,−15.7,−9.1) | 27.4 | (5.82,−12.44) |
| Castor MG | 200 | (−10.7,−8.0,−9.7) | 16.5 | (4.75,−18.44) |
| Ursa Major Group (Sirius Supercluster) | 300 | (14.9,1.0,−10.7) | 18.4 | (20.55,−38.10) |
| Hyades Supercluster (Hyades, Praesepe) | 600 | (−39.7,−17.7,−2.4) | 43.5 | (6.40,6.50) |



Downloaded from https://academic.oup.com/mnras/article/357/2/497/1370601 by Akdeniz University user on 20 September 2021

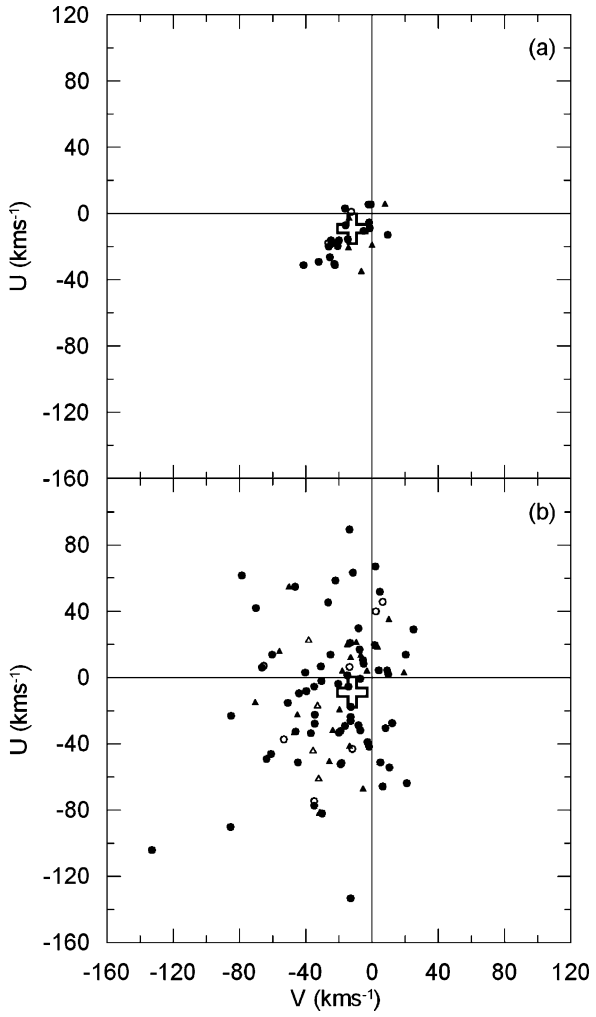


**Figure 7.** Distribution of (a) possible MGs and (b) FCBs on the ($U$, $V$) diagram. The position of the LSR is marked by a cross. The symbols are the same as in Fig. 1.

decrease in the binary evolution. A similar study is intended here to study the contact stage of the binary evolution. The physical parameters of W UMa binaries are listed in Table 5. The columns are self-explanatory to indicate order number, name, apparent brightness and colour ($B$–$V$), spectral type, binary type (A or W), orbital period and inclination, masses of components, mass ratio, and overcontact parameter $f$. The data were primarily collected from the same literature from which the radial velocities were taken. Moreover, the orbital inclinations and $f$ values are taken from Pribulla, Kreiner & Tremko (2003) and Selam (2004).

The distributions according to spectral types are compared between the MG (younger) and FCB group (older) in Fig. 8. It is interesting that both groups have a similar shape distribution. A slightly increased percentage of A-type stars in the MG appears to be the only difference. Fig. 9 compares the orbital period distributions between the MG and the FCB group. If one of the stars with an orbital period greater than 1 d in the MG is not counted, both groups cover nearly the same orbital period range ($0.2 < P < 0.9$ d). Both groups can be said to have a peak at $P = 0.4$ d. With 27 members, the MG has an average period $\langle P \rangle = 0.5258$ d. With 97 members, the FCB group has an average period $\langle P \rangle = 0.4275$ d. Comparing the shape of both histograms, we can conclude that the relative number of longer-period ($P > 0.4$ d) systems decreased and the relative number of shorter-period systems ($P < 0.4$ d) increased in the older population sample (the FCB group).

These changes may appear as evidence of the period decrease in the contact binary evolution. Karataş et al. (2004) assumed the period histogram of possible MG members as the initial period distribution of field CABs. However, here the situation is totally different. If the contact stage time-scale is indeed short as estimated to be within the range $0.1 < t_{\rm contact} < 1$ Gyr by Guinan & Bradstreet (1988), MG contact binaries cannot be taken as an initial distribution of the FCB group, because MG contact binaries will not be able to survive up to the mean kinematical age of the FCB group.

The mean kinematical age of the FCB group is 5.47 Gyr (Table 3). Karataş et al. (2004) assigned an age of 3.86 Gyr for the field CABs, which are potential progenitors of FCBs (Demircan 1999). Therefore, if there is a continuous formation of CABs and evolution out of the CAB stage, some (or maybe most) of these become W UMa systems; similarly, if the formation of W UMa systems and their evolution (coalescence) into a single star is a continuous process, and somehow if there is an equilibrium in the Galaxy, which could be investigated of course, the 1.61-Gyr age difference between field CABs and FCBs implies an upper limit for the time-scale of the contact stage. Indeed, it is not much different than the estimate of $0.1 < t_{\rm contact} < 1$ Gyr by Guinan & Bradstreet (1988).

Therefore, it is not possible to assume the MG to be the initial stage of the FCB group. It is most likely that the MG contact systems are formed in the beginning of the main sequence or during the pre-main-sequence contraction phase, either by a fission process (Roxburgh 1966) or most probably by fast spiralling in of two components in a common envelope. On the other hand, FCBs must be mostly formed from the detached progenitors.

The evidence of total mass and orbital period decrease appears to be better displayed in Table 6 where the FCBs are divided into four subgroups according to the orbital period criterion. It is clearly displayed there that the average kinematical age increases as the orbital periods of the subgroups decrease. It is also clear that older subgroups have smaller total mass. If long-period contact binaries in Table 6 lose mass and angular momentum, so their orbital period decreases within the time-scale indicated in the table. However, this scenario is definitely misleading and cannot be true. This is because the age difference between the youngest and oldest subgroups in Table 6 is too long for a contact system to survive, even if the empirical 1.61-Gyr time-scale for the contact stage were taken into consideration.

According to the true scenario, the large dispersions (older ages) in Table 6 must have been produced not only during the contact stage, but also including the pre-contact stages before, which may be longer than the contact stage, as indicated by Table 6. Thus, one should never expect, for a W UMa system in the youngest group in Table 6, to lose mass and angular momentum and join the shortest-period (oldest) W UMa systems $t = 8.89$–$3.21 = 5.68$ Gyr later. It is not yet clear, but it seems that when a detached system becomes a contact binary, the angular momentum loss becomes accelerated with the gravitational radiation, as described by Guinan & Bradstreet (1988). If the total mass of the system does not decrease to fit in the decreasing Roche lobes, then the overcontact $f$ parameter starts to increase. The pre-contact stage, which may differ from system to system, being much longer than the contact stage, spoils the correlation between the $f$ parameter and the space velocity, as described in Fig. 5.

Fig. 10 displays the total mass histograms of possible MG and FCB group. Similar to the period histograms, it would be meaningless to try to deduce evidence of mass decrease during contact



Downloaded from https://academic.oup.com/mnras/article/357/2/497/1370601 by Akdeniz University user on 20 September 2021

**Table 5.** Physical parameters of W UMas.

| ID | Name | $V$ | $B–V$ | Spectral type | Binary type | $P$ (d) | $i$ (°) | $M_1$ ($M_\odot$) | $M_2$ ($M_\odot$) | $q$ | $f$ | Third/multi-component |
|---|---|---|---|---|---|---|---|---|---|---|---|---|
| 1 | AQ Tuc | 9.91 | 0.35 | F2/5 | A | 0.5948 | 80.2 | 1.930 | 0.690 | 0.358 | 0.44 | |
| 2 | BH Cas | 12.30 | 1.02 | K4V | W | 0.4059 | 70.1 | 0.743 | 0.352 | 0.474 | 0.09 | |
| 3 | DZ Psc | 10.18 | 0.51 | F7V | A | 0.3661 | | | | 0.136 | | |
| 4 | V523 Cas | 10.62 | 1.05 | K4V | W | 0.2337 | 82.0 | 0.637 | 0.319 | 0.501 | 0.20 | √ |
| 5 | AQ Psc | 8.68 | 0.54 | F8V | A | 0.4756 | | | | 0.226 | | |
| 6 | AE Phe | 7.56 | 0.64 | F8V | W | 0.3624 | 85.3 | 1.366 | 0.629 | 0.461 | 0.17 | |
| 7 | TW Cet | 10.43 | 0.67 | G5V | W | 0.3117 | 83.2 | 1.284 | 0.680 | 0.530 | 0.03 | |
| 8 | V776 Cas | 8.94 | 0.52 | F2V | A | 0.4404 | 52.5 | 1.723 | 0.225 | 0.130 | 0.70 | |
| 9 | QX And | 11.25 | 0.44 | F5V | A | 0.4118 | 58.6 | 1.176 | 0.236 | 0.261 | 0.22 | |
| 10 | SS Ari | 10.37 | 0.62 | G0V | W | 0.4060 | 75.3 | 1.343 | 0.406 | 0.302 | 0.13 | √ |
| 11 | GZ And | 10.83 | 0.78 | G5V | W | 0.3050 | 85.9 | 1.170 | 0.602 | 0.514 | 0.03 | |
| 12 | V376 And | 7.68 | 0.26 | A4V | A | 0.7987 | | | | 0.305 | | |
| 13 | EE Cet | 8.76 | 0.36 | F2V | W | 0.3799 | 77.5 | 1.391 | 0.438 | 0.315 | 0.20 | |
| 14 | UX Eri | 10.50 | 0.67 | F9V | A | 0.4453 | 79.0 | 1.366 | 0.510 | 0.373 | 0.00 | |
| 15 | EQ Tau | 10.50 | 0.83 | G2V | A | 0.3413 | 86.6 | 1.217 | 0.537 | 0.442 | 0.12 | √ |
| 16 | BL Eri | 11.50 | 0.63 | G0V | W | 0.4169 | 88.0 | 0.609 | 0.330 | 0.542 | 0.16 | |
| 17 | YY Eri | 8.10 | 0.67 | G5V | W | 0.3215 | 82.5 | 1.540 | 0.620 | 0.403 | 0.12 | √ |
| 18 | AO Cam | 9.50 | 0.68 | G0V | W | 0.3299 | 75.1 | 1.189 | 0.491 | 0.413 | 0.10 | |
| 19 | RZ Tau | 10.08 | 0.58 | A7V | A | 0.4157 | 82.7 | 1.634 | 0.882 | 0.540 | 0.33 | |
| 20 | DN Cam | 8.23 | 0.34 | F2V | W | 0.4983 | 71.9 | 1.915 | 0.805 | 0.421 | 0.50 | |
| 21 | V410 Aur | 10.10 | 0.64 | G0/2V | A | 0.3663 | 90.0 | 1.234 | 0.178 | 0.144 | 0.50 | |
| 22 | V402 Aur | 8.84 | 0.40 | F2V | W | 0.6035 | | | | 0.201 | | |
| 23 | AP Dor | 9.38 | 0.45 | F5V | W | 0.4272 | 62.5 | | | 0.100 | 1.00 | |
| 24 | V1363 Ori | 10.30 | 0.58 | F8V | A | 0.4319 | | | | 0.205 | 0.40 | |
| 25 | ER Ori | 9.28 | 0.49 | F7V | W | 0.4234 | 87.5 | 1.385 | 0.765 | 0.552 | 0.15 | √ |
| 26 | RW Dor | 10.80 | 0.89 | K1V | W | 0.2854 | 76.6 | 0.640 | 0.430 | 0.672 | 0.10 | |
| 27 | V781 Tau | 8.90 | 0.57 | G0V | W | 0.3449 | 65.4 | 1.237 | 0.501 | 0.405 | 0.23 | |
| 28 | AH Aur | 10.20 | 0.55 | F7V | A | 0.4943 | 75.5 | 1.683 | 0.284 | 0.169 | 0.23 | |
| 29 | QW Gem | 10.33 | 0.48 | F8V | W | 0.3581 | 85.0 | 1.275 | 0.425 | 0.334 | 0.50 | |
| 30 | V753 Mon | 8.30 | 0.36 | A8V | W | 0.6770 | 74.0 | 1.673 | 1.623 | 0.970 | 0.00 | |
| 31 | TY Pup | 8.40 | 0.41 | F3V | A | 0.8192 | 81.6 | 2.200 | 0.720 | 0.327 | 0.63 | |
| 32 | FG Hya | 9.90 | 0.64 | G2V | A | 0.3278 | 86.8 | 1.414 | 0.157 | 0.112 | 0.74 | |
| 33 | TX Cnc | 10.00 | 0.42 | F8V | W | 0.3829 | 62.4 | 0.792 | 0.420 | 0.535 | 0.08 | |
| 34 | AH Cnc | 13.31 | 0.53 | F5V | W | 0.3604 | 68.0 | 1.290 | 0.540 | 0.419 | 0.41 | |
| 35 | UV Lyn | 9.41 | 0.64 | F6V | W | 0.4150 | 66.8 | 1.349 | 0.495 | 0.367 | 0.45 | |
| 36 | FN Cam | 8.58 | 0.38 | A9V | A | 0.6771 | 71.2 | 2.402 | 0.532 | 0.222 | 0.56 | |
| 37 | EZ Hya | 10.48 | 0.82 | G2V | W | 0.4498 | | | | 0.252 | | |
| 38 | S Ant | 6.40 | 0.36 | A9V | A | 0.6483 | 68.8 | 1.940 | 0.760 | 0.392 | 0.07 | |
| 39 | W UMa | 7.75 | 0.62 | F8V | W | 0.3336 | 86.0 | 1.190 | 0.570 | 0.479 | 0.32 | |
| 40 | AA UMa | 10.88 | 0.60 | F9V | W | 0.4680 | 80.3 | 1.419 | 0.773 | 0.545 | 0.15 | |
| 41 | RT Lmi | 11.40 | 0.60 | F7V | A | 0.3749 | 84.0 | 1.298 | 0.476 | 0.367 | 0.23 | |
| 42 | XY Leo | 9.45 | 1.04 | K0V | W | 0.2841 | 65.8 | 0.870 | 0.435 | 0.500 | 0.06 | √ |
| 43 | XZ Leo | 10.60 | 0.38 | A8V | A | 0.4877 | 73.3 | 1.892 | 0.659 | 0.348 | 0.02 | |
| 44 | Y Sex | 9.02 | 0.48 | F8 | A | 0.4198 | 76.8 | 1.210 | 0.220 | 0.182 | 0.00 | |
| 45 | ET Leo | 9.55 | 0.62 | G8V | W | 0.3465 | 47.5 | 0.835 | 0.285 | 0.342 | 0.10 | |
| 46 | UZ Leo | 9.58 | 0.39 | A9V | A | 0.6180 | 79.7 | 2.074 | 0.629 | 0.303 | 0.85 | |
| 47 | EX Leo | 8.27 | 0.53 | F6V | A | 0.4086 | 61.1 | 1.557 | 0.309 | 0.199 | 0.31 | |
| 48 | VY Sex | 9.02 | 0.55 | F9.5 | W | 0.4434 | | | | 0.313 | | |
| 49 | AM Leo | 9.25 | 0.56 | F5V | W | 0.3658 | 87.0 | 1.386 | 0.623 | 0.449 | 0.15 | √ |
| 50 | VW Lmi | 8.03 | 0.41 | F3V | A | 0.4775 | 72.5 | | | 0.250 | 0.40 | |
| 51 | AP Leo | 9.32 | 0.50 | F8V | A | 0.4304 | 77.0 | 1.477 | 0.439 | 0.297 | 0.23 | |
| 52 | HN UMa | 9.90 | 0.59 | F8V | A | 0.3826 | | | | 0.140 | 0.20 | |
| 53 | AW UMa | 6.84 | 0.37 | F2V | A | 0.4387 | 79.8 | 1.280 | 0.090 | 0.070 | 0.85 | √ |
| 54 | TV Mus | 11.00 | 0.82 | F8V | A | 0.4457 | 78.9 | 1.316 | 0.157 | 0.119 | 0.87 | |
| 55 | V752 Cen | 9.17 | 0.58 | F7V | W | 0.3702 | 81.7 | 1.320 | 0.410 | 0.311 | 0.06 | |
| 56 | AG Vir | 8.35 | 0.29 | A8V | A | 0.6427 | 80.7 | 1.610 | 0.510 | 0.317 | | |
| 57 | HX UMa | 8.89 | 0.49 | F4V | A | 0.3792 | 50.0 | 1.333 | 0.387 | 0.291 | 0.70 | |
| 58 | CC Com | 11.30 | 1.24 | K5V | W | 0.2211 | 90.0 | 0.690 | 0.360 | 0.522 | 0.20 | |
| 59 | AH Vir | 8.89 | 0.81 | G8V | W | 0.4075 | 86.5 | 1.360 | 0.412 | 0.303 | 0.24 | √ |
| 60 | II UMa | 8.17 | 0.61 | F5III | A | 0.8250 | 70.0 | 2.238 | 0.385 | 0.172 | 0.70 | |
| 61 | RW Com | 11.07 | 0.84 | K0V | W | 0.2373 | 75.2 | 0.920 | 0.310 | 0.337 | 0.17 | |
| 62 | RZ Com | 10.42 | 0.52 | F8V | W | 0.3385 | 86.0 | 1.108 | 0.484 | 0.437 | 0.07 | |

Downloaded from https://academic.oup.com/mnras/article/357/2/497/1370601 by Akdeniz University user on 20 September 2021

**Table 5** – *continued*

| ID | Name | $V$ | $B$–$V$ | Spectral type | Binary type | $P$ (d) | $i$ (°) | $M_1$ ($M_\odot$) | $M_2$ ($M_\odot$) | $q$ | $f$ | Third/multi-Component |
|---|---|---|---|---|---|---|---|---|---|---|---|---|
| 63 | SX Crv | 9.07 | 0.56 | F6V | A | 0.3166 | | | | 0.066 | | |
| 64 | BI CVn | 10.26 | 0.62 | F2V | A | 0.3842 | 69.2 | 1.646 | 0.679 | 0.413 | 0.17 | |
| 65 | KZ Vir | 8.45 | 0.47 | F7V | A | 1.1318 | | | | 0.848 | | |
| 66 | KR Com | 7.26 | 0.57 | G0IV | A | 0.4080 | | | | 0.091 | 0.70 | |
| 67 | HT Vir | 7.06 | 0.56 | F8V | A | 0.4077 | 90.0 | 1.258 | 1.022 | 0.812 | | |
| 68 | XY Boo | 10.30 | 0.49 | F5V | A | 0.3706 | 69.0 | 0.934 | 0.147 | 0.158 | 0.05 | |
| 69 | V757 Cen | 8.30 | 0.64 | F9V | W | 0.3432 | 69.3 | 1.000 | 0.690 | 0.690 | 0.14 | |
| 70 | RR Cen | 7.27 | 0.34 | A9V | A | 0.6057 | 78.7 | 1.854 | 0.389 | 0.210 | 0.35 | |
| 71 | VW Boo | 10.50 | 0.81 | G5V | W | 0.3422 | 76.2 | 0.980 | 0.420 | 0.428 | 0.72 | |
| 72 | NN Vir | 7.64 | 0.41 | F0/F1V | A | 0.4807 | 65.0 | 1.794 | 0.882 | 0.491 | 0.50 | |
| 73 | EF Boo | 9.43 | 0.50 | F5V | W | 0.4295 | 75.2 | 1.554 | 0.795 | 0.512 | 0.20 | |
| 74 | CK Boo | 8.99 | 0.54 | F7/8V | A | 0.3552 | 56.6 | 1.788 | 0.198 | 0.111 | 0.14 | |
| 75 | GR Vir | 7.80 | 0.58 | F7/8V | A | 0.3470 | | | | 0.122 | | |
| 76 | AC Boo | 10.00 | 0.59 | F8Vn | W | 0.3524 | 82.6 | 1.403 | 0.565 | 0.403 | 0.91 | |
| 77 | TY Boo | 10.81 | 0.76 | G5V | W | 0.3171 | 76.6 | 0.930 | 0.400 | 0.437 | 0.10 | ✓ |
| 78 | 44 Boo | 5.80 | 0.85 | K2V | W | 0.2678 | 72.8 | 0.900 | 0.439 | 0.487 | 0.00 | ✓ |
| 79 | TZ Boo | 10.41 | 0.63 | G2V | A | 0.2972 | 66.9 | 0.783 | 0.104 | 0.133 | | |
| 80 | BW Dra | 8.61 | 0.63 | F8V | W | 0.2923 | 74.4 | 0.891 | 0.250 | 0.281 | 0.14 | |
| 81 | BV Dra | 7.88 | 0.56 | F7V | W | 0.3501 | 76.3 | 0.997 | 0.401 | 0.402 | 0.11 | |
| 82 | FI Boo | 9.60 | 0.72 | G3V | W | 0.3900 | | | | 0.372 | 0.10 | |
| 83 | OU Ser | 8.25 | 0.64 | F9/G0V | A | 0.2968 | 74.3 | 1.018 | 0.176 | 0.173 | 0.31 | |
| 84 | VZ Lib | 10.13 | 0.64 | G0 | A | 0.3583 | | | | 0.237 | | |
| 85 | FU Dra | 10.55 | 0.59 | F8V | W | 0.3067 | 78.6 | 1.168 | 0.293 | 0.251 | 0.23 | |
| 86 | YY CrB | 8.64 | 0.62 | F8V | A | 0.3766 | 77.0 | 1.429 | 0.348 | 0.243 | 0.63 | |
| 87 | AU Ser | 10.90 | 0.87 | K0V | A | 0.3865 | 80.6 | 0.921 | 0.646 | 0.701 | 0.09 | |
| 88 | V842 Her | 9.85 | 0.65 | F9V | W | 0.4190 | 79.0 | 1.360 | 0.353 | 0.260 | 0.25 | |
| 89 | BX Dra | 10.50 | 0.35 | F0IV-V | A | 0.5790 | | | | 0.289 | | |
| 90 | V899 Her | 7.93 | 0.45 | F5V | A | 0.4212 | 68.7 | 1.836 | 1.039 | 0.566 | 0.30 | |
| 91 | V502 Oph | 8.34 | 0.65 | G0V | W | 0.4534 | 71.3 | 1.297 | 0.481 | 0.335 | 0.24 | ✓ |
| 92 | V918 Her | 7.30 | 0.28 | A7V | W | 0.5748 | | | | 0.271 | | |
| 93 | V921 Her | 9.44 | 0.39 | A7IV | A | 0.8774 | 87.5 | 1.609 | 0.365 | 0.226 | 0.20 | |
| 94 | V829 Her | 10.10 | 0.65 | G2V | W | 0.3582 | 57.0 | 1.275 | 0.520 | 0.408 | | |
| 95 | V2357 Oph | 10.67 | 0.86 | G5V | A | 0.4156 | | | | 0.231 | 0.40 | |
| 96 | AK Her | 8.29 | 0.55 | F5V | A | 0.4215 | 80.8 | 1.310 | 0.300 | 0.229 | 0.10 | ✓ |
| 97 | V728 Her | 10.90 | 0.41 | F3V | W | 0.4713 | 69.2 | 1.654 | 0.295 | 0.178 | 0.71 | |
| 98 | GM Dra | 8.77 | 0.51 | F5V | W | 0.3387 | | | | 0.180 | 0.40 | |
| 99 | V2377 Oph | 8.60 | 0.66 | G0/1V | W | 0.4254 | | | | 0.395 | 0.80 | |
| 100 | V535 Ara | 7.17 | 0.34 | A8V | A | 0.6293 | 82.1 | 1.520 | 0.460 | 0.303 | 0.03 | |
| 101 | V2388 Oph | 6.25 | 0.47 | F3V | A | 0.8023 | 83.9 | 1.648 | 0.306 | 0.186 | 0.71 | |
| 102 | V566 Oph | 7.46 | 0.45 | F4V | A | 0.4096 | 79.8 | 1.469 | 0.357 | 0.243 | 0.41 | |
| 103 | V972 Her | 6.72 | 0.47 | F4V | W | 0.4431 | | | | 0.167 | 0.00 | |
| 104 | V508 Oph | 10.06 | 0.67 | F9V | A | 0.3448 | 86.1 | 1.010 | 0.520 | 0.515 | 0.10 | |
| 105 | EF Dra | 10.48 | 0.82 | F9V | A | 0.4240 | 78.1 | 1.813 | 0.289 | 0.160 | 0.45 | ✓ |
| 106 | V839 Oph | 8.80 | 0.62 | F7V | A | 0.4090 | 80.1 | 1.640 | 0.496 | 0.305 | 0.39 | |
| 107 | eps Cra | 4.74 | 0.40 | F2V | A | 0.5914 | 72.3 | 1.720 | 0.220 | 0.128 | 0.30 | |
| 108 | V401 Cyg | 10.64 | 0.38 | F0V | A | 0.5827 | 77.0 | 1.679 | 0.487 | 0.290 | 0.46 | |
| 109 | V2082 Cyg | 6.68 | 0.35 | F2V | A | 0.7141 | | | | 0.238 | | |
| 110 | V417 Aql | 11.00 | 0.53 | G2V | W | 0.3703 | 84.5 | 1.395 | 0.505 | 0.362 | 0.19 | |
| 111 | OO Aql | 9.20 | 0.61 | G2V | A | 0.5068 | 90.0 | 1.040 | 0.880 | 0.846 | 0.27 | |
| 112 | VW Cep | 7.23 | 0.86 | G9V | W | 0.2783 | 63.6 | 0.897 | 0.247 | 0.275 | 0.22 | ✓ |
| 113 | LS Del | 8.61 | 0.68 | G0V | W | 0.3638 | 48.5 | 1.068 | 0.399 | 0.375 | 0.06 | |
| 114 | V2150 Cyg | 8.09 | 0.40 | A6V | A | 0.5919 | | | | 0.802 | 0.90 | |
| 115 | HV Aqr | 9.71 | 0.63 | F5V | A | 0.3745 | 78.3 | 1.366 | 0.198 | 0.145 | 0.47 | |
| 116 | V1073 Cyg | 8.23 | 0.45 | F2V | A | 0.7859 | 68.4 | 1.600 | 0.510 | 0.319 | 0.04 | |
| 117 | KP Peg | 7.07 | 0.16 | A2V | A | 0.7272 | | | | 0.322 | | |
| 118 | DK Cyg | 10.37 | 0.39 | A8V | A | 0.4707 | 80.3 | 1.768 | 0.575 | 0.325 | 0.55 | |
| 119 | BX Peg | 11.00 | 0.78 | G4.5 | W | 0.2804 | 87.5 | 1.020 | 0.380 | 0.373 | 0.18 | |
| 120 | V445 Cep | 6.85 | 0.14 | A2V | A | 0.4488 | | | | 0.167 | | |
| 121 | BB Peg | 10.80 | 0.52 | F5V | W | 0.3615 | 79.9 | 1.431 | 0.515 | 0.360 | 0.37 | |
| 122 | V335 Peg | 7.24 | 0.50 | F5V | A | 0.8107 | | | | 0.262 | 0.10 | |
| 123 | SW Lac | 8.51 | 0.75 | K0Vvar | W | 0.3207 | 80.2 | 0.959 | 0.779 | 0.851 | 0.39 | ✓ |
| 124 | AB And | 9.50 | 0.87 | G8V | W | 0.3319 | 86.8 | 1.005 | 0.494 | 0.560 | 0.15 | ✓ |

Downloaded from https://academic.oup.com/mnras/article/357/2/497/1370601 by Akdeniz University user on 20 September 2021

**Table 5** – *continued*

| ID | Name | $V$ | $B–V$ | Spectral type | Binary type | $P$ (d) | $i$ (°) | $M_1$ ($M_\odot$) | $M_2$ ($M_\odot$) | $q$ | $f$ | Third/multi-Component |
|---|---|---|---|---|---|---|---|---|---|---|---|---|
| 125 | V351 Peg | 8.00 | 0.34 | A8V | W | 0.5933 | 62.5 | 2.327 | 0.838 | 0.360 | 0.40 | |
| 126 | VZ Psc | 10.20 | 1.14 | K5V | A | 0.2613 | 49.6 | 0.790 | 0.720 | 0.911 | 0.00 | |
| 127 | BD +14 5016 | 9.50 | 0.31 | F0V | A | 0.6369 | 72.6 | 1.531 | 0.387 | 0.253 | 0.54 | |
| 128 | EL Aqr | 10.49 | 0.50 | F3V | A | 0.4814 | 70.8 | 1.563 | 0.317 | 0.203 | | |
| 129 | U Peg | 9.23 | 0.62 | G2V | W | 0.3748 | 77.5 | 1.149 | 0.379 | 0.330 | 0.09 | |

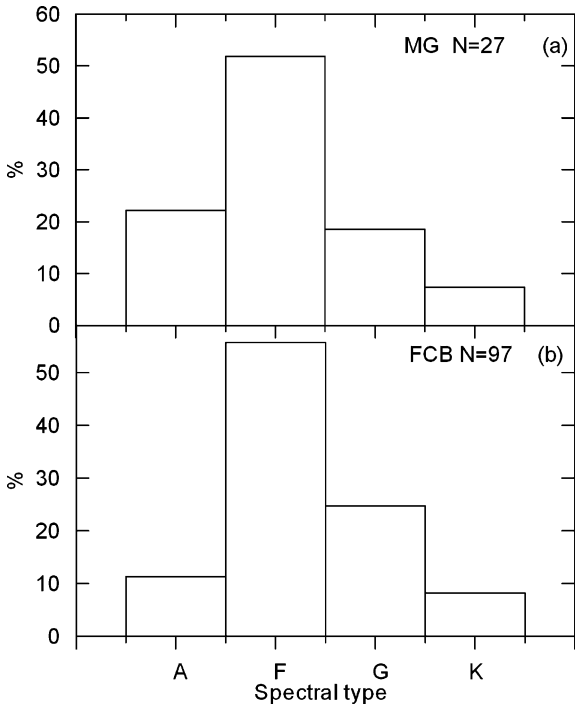


**Figure 8.** Comparison of spectral-type histograms of (a) MGs and (b) FCBs.

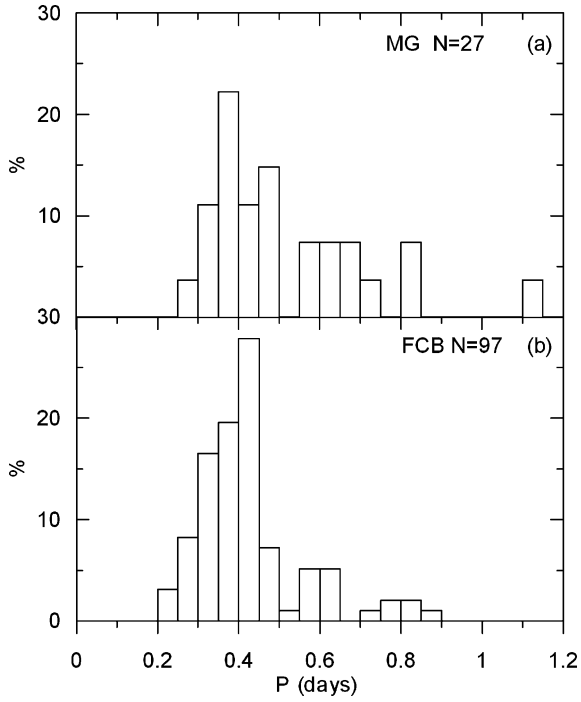


**Figure 9.** Comparison of period histograms of (a) MGs and (b) FCBs.

binary evolution from this figure. Therefore, it should be considered as a bare comparison between the MG and the FCB group. It is the same with Fig. 11, which compares the mass ratio distribution between the MG and the FCB group. The mass ratio evolution during the contact stage cannot be deduced from Fig. 11 because the MG cannot be the initial distribution. On the other hand, all four histograms (Figs 8–11) display empirical evidence of contact binary evolution to indicate the coalescence of W UMa systems into single stars. Otherwise, angular momentum loss does not fit into the theory of binary evolution. Then, it becomes difficult to explain why there are such differences between the MG and the FCB group W UMa stars.

A similar case also applies to the data of Table 6. We believe the age difference between MG contact binaries and the youngest FCB group in Table 6 is empirical evidence of coalescence into single stars. This is because the coalescence into a single star involves orbital period decrease as well as angular momentum loss, most probably accelerated by gravitational radiation, as described by Guinan & Bradstreet (1988), although the data in Table 6 are mostly affected by the long pre-contact stages. The derivation of the rates of orbital period decrease, mass and angular momentum loss from the present data of contact binaries requires a careful analysis and interpretation of the data of Table 6. Due to limited space in this paper, the derivation of these rates will be handled in a forthcoming study.

**Table 6.** Kinematical ages for the period subgroups in the FCB group.

| $P$ (d) | $\langle M_{\rm tot}\rangle$ ($M_\odot$) | $\langle P\rangle$ (d) | N | $\sigma_{\rm tot}$ (km s$^{-1}$) | Age (Gyr) |
|---|---|---|---|---|---|
| (0.5–0.9] | 2.220 | 0.669 | 17 | 42.09 7.1 | 3.21 |
| (0.4–0.5] | 1.900 | 0.434 | 34 | 43.86 10.4 | 3.51 |
| (0.3–0.4] | 1.618 | 0.353 | 35 | 63.90 16.0 | 7.14 |
| (0.2–0.3] | 1.171 | 0.270 | 11 | 73.92 14.6 | 8.89 |

## 5 CONCLUSION

We have studied the kinematics of 129 W UMa binaries. The sample is found to be heterogeneous in the velocity space, i.e. kinematically younger and older contact binaries exist in the present sample. Various subgroups are formed according to criteria involving the spectral type, binary type (A or W), mass ratio and overcontact parameter $f$, orbital period and total mass. However, these criteria failed to produce kinematically homogeneous subgroups. Nevertheless, a correlation has been found to indicate that shorter-period less-massive



Downloaded from https://academic.oup.com/mnras/article/357/2/497/1370601 by Akdeniz University user on 20 September 2021

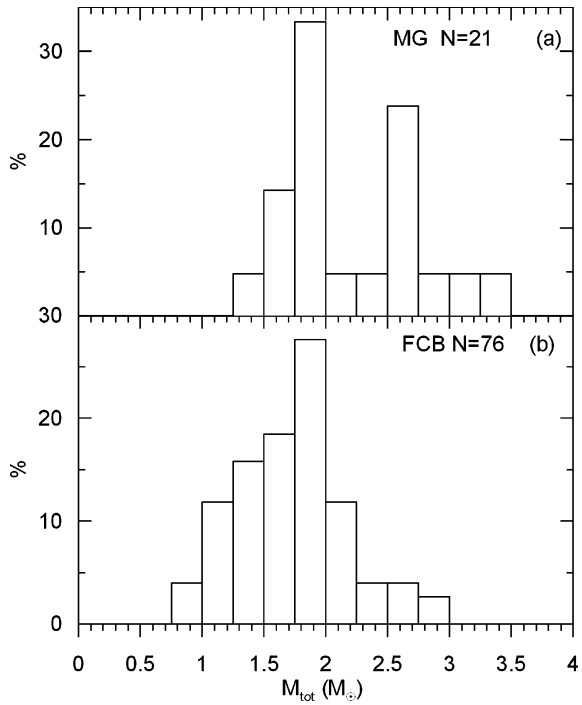


**Figure 10.** Comparison of the total mass ($M_h + M_c$) histograms of (a) MGs and (b) FCBs.

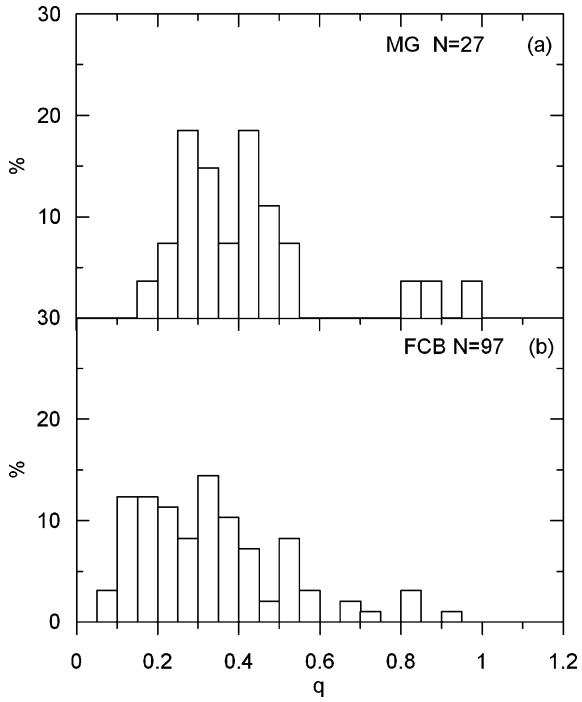


**Figure 11.** Comparison of the mass ratio ($q = M_2/M_1$, where $M_2 < M_1$, and $M_1$ and $M_2$ are the primary and secondary masses, respectively) histograms of (a) MGs and (b) FCBs.

systems show larger velocity dispersions than longer-period more-massive systems. The mean kinematical ages of all subgroups are estimated from the velocity dispersions using the tables of Wielen (1982), and are listed in Table 3.

The possible MG members among the present W UMa stars are investigated according to the kinematical criteria originally defined by Eggen (1958a,b, 1989, 1995), and 28 W UMa are found to be possible members of the five best-documented MGs, which are summarized in Table 4. The FCB group is formed by removing the possible MG members and the W UMa systems that are known to be members of known open clusters from the main sample. The 5.47-Gyr mean kinematical age is estimated for the FCBs. The age difference is found to be 1.61 Gyr between the 3.86-Gyr-old CABs (Karataş et al. 2004) and the FCB group. If there is a number equilibrium between the CAB and FCB groups established by the evolution, the upper limit of the lifetime of the contact stage can be estimated as 1.61 Gyr, which is in close agreement with the estimation made by Guinan & Bradstreet (1988), $0.1 < t_{\rm contact} < 1$ Gyr.

Because the contact stage appears to be very short in comparison with the mean kinematical age of the FCB group, the group containing possible MG stars cannot be used as an initial subsample of the FCB group. Thus, the histograms (Figs 8–10) and ages of the subgroups of the FCB group according to orbital ranges (Table 6) cannot be used directly to deduce evidence of period decrease and angular momentum loss during contact stage evolution. Nevertheless, because these histograms and the data in Table 6 cannot be explained without angular momentum loss and orbital period decrease in binary evolution, and because it is illogical to assume that angular momentum loss and orbital period decrease operate only for the pre-contact stages, the angular momentum loss and the orbital period decrease are evidently occurring, as predicted by Guinan & Bradstreet (1988), even if we cannot deduce them directly from these histograms and Table 6.

We have found 27 systems to form the MG. The existence of MG members is an exciting (perhaps the most exciting) finding of this study. This is because these W UMa systems are not old enough to be formed from detached binary progenitors by the mechanism involving angular momentum loss and orbital period decrease. In fact, the age difference between the youngest FCB subgroup (3.21 Gyr, in Table 6) and the MG (0.5 Gyr, in Table 3) is more than the lifetime (1.61 Gyr) of the contact stage. Therefore, it can be concluded that the MG contact systems are formed in the beginning of the main sequence or during the pre-main-sequence contraction phase, either by a fission process (Roxburgh 1966) or by fast spiralling in of the two components in a common envelope. As a result, it can be said that detached binary progenitors, presumably short-period ($P < 5$ d) RS CVn binaries, are not the only source from which W UMa systems could be formed by the mechanism involving angular momentum loss and orbital period decrease. It is indeed a challenge to disprove true membership of MG stars in our list. This may not be enough; we also need to prove that their ages are greater than our estimate, that is, their ages must be proven to be big enough (bigger than the pre-main-sequence contraction plus the contact stage lifetime). Then, we can claim that detached binary progenitors are the only source to form W UMa systems.

## ACKNOWLEDGMENTS

This research has made use of the SIMBAD data base, operated at CDS, Strasbourg, France. Thanks to B. J. Hrivnak for providing private communications. We also thank the referee, Dr Slavek Rucinski, for his substantial input into the paper. A British national, who is an English teacher, Margaret Kadıoğlu helped with the grammar and linguistics. This work was supported by the Research Fund of the University of Istanbul, project number 244/23082004.



Downloaded from https://academic.oup.com/mnras/article/357/2/497/1370601 by Akdeniz University user on 20 September 2021

## REFERENCES


Ahn Y. S., Hill G., Khalesseh B., 1992, A&A, 265, 597
Aslan Z., Özdemir T., Yeşilyaprak C., İskender A., 1999, Turkish J. Phys., 23, 45
Bartkevicius A., Lazauskaite R., Bartasiute S., 1999, in D. Egret, A. Heck, eds, ASP Conf. Ser. Vol. 167, Harmonizing Cosmic Distance Scales in a Post-*Hipparcos* Era. Astron. Soc. Pac., San Francisco, p. 247
Batten A. H., Lu W., 1986, PASP, 98, 92
Bell S. A., Rainger P. P., Hilditch R. W., 1990, MNRAS, 247, 632
Binnendijk L., 1970, Vistas in Astronomy, 12, 217
Bopp B. W., Rucinski S. M., 1981, in Sugimoto D. et al., eds, Proc. IAU Symp. 93, Fundamental Problems in the Theory of Stellar Evolution. Reidel, Dordrecht, p. 177
Bopp B. W., Stencel R. E., 1981, ApJ, 247, L131
Buser R., Rong J., Karaali S., 1999, A&A, 348, 98
Cerruti M. A., Niemela V. S., 1982, PASP, 94, 195
Demircan O., 1999, Tr. J. Phys., 23, 425
Duerbeck H. W., 1978, Acta Astron., 28, 49
Eggen O. J., 1958a, MNRAS, 118, 65
Eggen O. J., 1958b, MNRAS, 118, 154
Eggen O. J., 1989, PASP, 101, 366
Eggen O. J., 1994, in Morrison L. V., Gilmore G., eds, Galactic and Solar System Optical Astrometry. Cambridge Univ. Press, Cambridge, p. 191
Eggen O. J., 1995, AJ, 110, 2862
Eker Z., 1992, ApJS, 79, 481
ESA, 1997, ESA SP-1200, The *Hipparcos* and Tycho Catalogues. ESA Publications Division, Noordwijk
Gatewood G., 1995, ApJ, 445, 712
Gatewood G., de Jonge J. K., 1994, ApJ, 428, 166
Goecking K. D., Duerbeck H. W., 1993, A&A, 278, 463
Goecking K. D., Duerbeck H. W., Plewa T., Kaluzny J., Schertl D., Weigelt G., Flin P., 1994, A&A, 289, 827
Green E. M., Demarque P., King C. R., 1987, The Revised Yale Isochrones. Yale Univ. Obs., New Haven
Grenon M., 1987, JA&Ap, 8, 123
Guinan E. F., Bradstreet D. H., 1988, in Dupree A. K., Lago M. T., eds, Formation and Evolution of Low Mass Stars. Kluwer, Dordrecht, p. 345
Hilditch R. W., King D. J., 1986, MNRAS, 223, 581
Hilditch R. W., King D. J., McFarlane T. M., 1989, MNRAS, 237, 447
Hilditch R. W., Hill G., Bell S. A., 1992, MNRAS, 255, 285
Hill G., 1989, A&A, 218, 141
Hill G., Barnes J. V., 1972, PASP, 84, 382
Hill G., Fisher W. A., Holmgren D., 1989, A&A, 218, 152
Hog E., Kuzmin A., Bastian U., Fabricius C., Kuimov K., Lindegren L., Makarov V. V., Roeser S., 1998, A&A, 335, L65
Hog E. et al., 2000, A&A, 355, L27
Hrivnak J., 1989, ApJ, 340, 458
Hrivnak B. J., 1993, in Leung K-C., Nha I-S., eds, ASP Conf. Ser. Vol. 38, New Frontiers in Binary Star Research: Pacific Rim Colloquium. Astron. Soc. Pac., San Francisco, p. 269
Hrivnak B. J., Milone E. F., 1989, AJ, 97, 523
Hrivnak B. J., Milone E. F., Hill G., Fisher W. A., 1984, ApJ, 285, 683
Huang S. S., 1967, ApJ, 150, 229
Jeffries R. D., 1995, MNRAS, 273, 559
Johnson D. R. H., Soderblom D. R., 1987, AJ, 93, 864
Joy A. H., 1926, ApJ, 64, 287
Karataş Y., Bilir S., Eker Z., Demircan O., 2004, MNRAS, 349, 1069
Karaali S., Bilir S., Hamzaoğlu E., 2004, MNRAS, 355, 307
King D. J., Hilditch R. W., 1984, MNRAS, 209, 645
King J. R., Villarreal A. R., Soderblom D. R., Gulliver A. F., Adelman, S. J., 2003, AJ, 125, 1980
Kukarkin B. V., Kholopov P. N., Pskovsky Y. K., Efremov Y. N., Kukarkina N. P., Kurochkin N. E., Medvedeva G. I., 1971, Third General Catalogue of Variable Stars, 3rd edn. Sternberg State Astron. Inst., Moscow
Lu W., 1985, PASP, 97, 1086
Lu W., 1986, PASP, 98, 577
Lu W., 1988a, Acta Astrophys. Sinica, 8, 26
Lu W., 1988b, Acta Astrophys. Sinica, 8, 259
Lu W., 1991, AJ, 102, 262
Lu W., 1993, AJ, 105, 646
Lu W., Rucinski S. M., 1993, AJ, 106, 361
Lu W., Rucinski S. M., 1999, AJ, 118, 515
Lu W., Rucinski S. M., Ogloza W., 2001, AJ, 122, 402
Maceroni C., 1986, A&A, 170, 43
Maceroni C., van't Veer F., 1996, A&A, 311, 523
Maciejewski G., Ligeza P., Karska A., 2003, Inf. Bull. on Variable Stars, 5400, 1
McLean B. J., 1981, MNRAS, 195, 931
McLean B. J., 1983, MNRAS, 204, 817
McLean B. J., Hilditch R. W., 1983, MNRAS, 203, 1
Marsakov V. A., Shevelev Y. G., 1995, Bull. Inf. Centre Donnees Stellaires, 47, 13
Mestel L., 1968, MNRAS, 138, 359
Metcalfe T. S., 1999, AJ, 117, 2503
Mihalas D., Binney J., 1981, Galactic Astronomy: Structure and Kinematics, 2nd edn. W. H. Freeman, San Francisco
Milone E. F., Hrivnak B. J., Hill G., Fisher W. A., 1985a, AJ, 90, 109
Milone E. F., Hrivnak B. J., Fisher W. A., 1985b, AJ, 90, 354
Milone E. F., Stagg C. R., Sugars B. A., McVean J. R., Schiller S. J., Kallrath J., Bradstreet D. H., 1995, AJ, 109, 359
Montes D., Lopez-Santiago J., Galvez M. C., Fernandez-Figueroa M. J., De Castro E., Cornide M., 2001a, MNRAS, 328, 45
Montes D., Fernandez-Figueroa M. J., De Castro E., Cornide M., Latorre A., 2001b, in R. J. Garcia Lopez, R. Rebolo, M. R. Zapaterio Osorio, eds, ASP Conf. Ser. Vol. 223, 11th Cambridge Workshop on Cool Stars, Stellar Systems and the Sun. Astron. Soc. Pac., San Francisco, p. 1477
Moore J. H., Paddock G. F., 1950, ApJ, 112, 48
Montgomery K. A., Marschall L. A., Janes K. A., 1993, AJ, 106, 181
Nelson R. H., Milone E. F., Vanleeuwen J., Terrell D., Penfold J. E., Kallrath J., 1995, AJ, 110, 2400
Nesci R., Maceroni C., Milano L., Russo G., 1986, A&A, 159, 142
Nordström B. et al., 2004, A&A, 418, 989
Okamoto I., Sato K., 1970, PASJ, 22, 317
Pazhouhesh R., Edalati M. T., 2003, Ap&SS, 288, 259
Perryman M. A. C. et al., 1997, A&A, 323L, 49
Plavec M., 1968, Adv. Astron. Astrophys., 6, 201
Pribulla T., Kreiner J. M., Tremko J., 2003, Coska, 33, 38
Przybylski A., Morris K. P., 1965, MNRAS, 129, 63
Pych W. et al., 2004, AJ, 127, 1712
Rainger P. P., Hilditch R. W., Bell S. A., 1990a, MNRAS, 246, 42
Rainger P. P., Bell S. A., Hilditch R. W., 1990b, MNRAS, 246, 47
Roese S., Bastian U., 1988, A&AS, 74, 449
Roxburgh I. W., 1966, ApJ, 143, 111
Rucinski S. M., 2004, NewAR, 48, 703
Rucinski S. M., Lu W., 1999, AJ, 118, 2451
Rucinski S. M., Whelan J. A. J., Worden S. P., 1977, PASP, 89, 684
Rucinski S. M., Lu W. X., Shi J., 1993, AJ, 106, 1174
Rucinski S. M., Lu W., Mochnacki S. W., 2000, AJ, 120, 1133
Rucinski S. M., Lu W., Mochnacki S. W., Ogloza W., Stachowski G., 2001, AJ, 122, 1974
Rucinski S. M., Lu W., Capobianco C. C., Mochnacki S. W., Blake R. M., Thomson J. R., Ogloza W., Stachowski G., 2002, AJ, 124, 1738
Rucinski S. M. et al., 2003, AJ, 125, 3258
Samec R. G., Hube D. P., 1991, AJ, 102, 1171
Sanford R. F., 1934, ApJ, 79, 89
Schoeffel E., 1979, A&AS, 36, 287
Selam S. O., 2004, A&A, 416, 1097
Siegel M. H., Majewski S. R., Reid I. N., Thompson I. B., 2002, ApJ, 578, 151
Sistero R. F., Castore de Sistero M. E., 1974, AJ, 79, 391
Struve O., 1950, ApJ, 112, 184
Struve O., Horak H. G., Canavaggia R., Kourganoff V., Colacevich A., 1950, ApJ, 111, 658
Thomas H. S., 1977, ARA&A, 15, 127


Downloaded from https://academic.oup.com/mnras/article/357/2/497/1370601 by Akdeniz University user on 20 September 2021

van't Veer F., 1975, A&A, 40, 167
van't Veer F., 1979, A&A, 80, 287
Vilhu O., Rahunen T., 1980, in Plavec M. J., Popper D. M., Ulrich D. R., eds, Proc. IAU Symp. 88, Close Binary Stars. Reidel, Dordrecht, p. 491
Whelan J. A. J., Romanishin W., Worden S. P., Rucinski S. M., 1979, MNRAS, 186, 729
Wielen R., 1982, Numerical Data and Functional Relationships in Science and Technology. Springer-Verlag, Berlin, p. 29
Yamasaki A., Jugaku J., Seki M., 1988, AJ, 95, 894
Zhai D., Lu W., 1989, Acta Astrophys. Sinica, 9, 208

This paper has been typeset from a TEX/LATEX file prepared by the author.

Downloaded from https://academic.oup.com/mnras/article/357/2/497/1370601 by Akdeniz University user on 20 September 2021